IMMUNOLOGY

Control of TLR7-mediated type I IFN signaling in pDCs through CXCR4 engagement—A new target for lupus treatment

Nikaïa Smith[1,2,3,4]*, Mathieu P. Rodero[1,2,3], Nassima Bekaddour[1,2,3], Vincent Bondet[5,6], Yasser B. Ruiz-Blanco[7], Mirja Harms[4], Benjamin Mayer[8], Brigitte Bader-Meunier[3,9,10,11], Pierre Quartier[3,9,10], Christine Bodemer[3,9,12], Véronique Baudouin[13], Yannick Dieudonné[14,15,16], Frank Kirchhoff[4], Elsa Sanchez Garcia[7], Bruno Charbit[17], Nicolas Leboulanger[3,18], Bernd Jahrsdörfer[19], Yolande Richard[3,20,21], Anne-Sophie Korganow[14,15,16], Jan Münch[4], Sébastien Nisole[22], Darragh Duffy[5,6,17], Jean-Philippe Herbeuval[1,2,3]*

Type I interferons are highly potent cytokines essential for self-protection against tumors and infections. Deregulations of type I interferon signaling are associated with multiple diseases that require novel therapeutic options. Here, we identified the small molecule, IT1t, a previously described CXCR4 ligand, as a highly potent inhibitor of Toll-like receptor 7 (TLR7)–mediated inflammation. IT1t inhibits chemical (R848) and natural (HIV) TLR7-mediated inflammation in purified human plasmacytoid dendritic cells from blood and human tonsils. In a TLR7-dependent lupus-like model, in vivo treatment of mice with IT1t drives drastic reduction of both systemic inflammation and anti–double-stranded DNA autoantibodies and prevents glomerulonephritis. Furthermore, IT1t controls inflammation, including interferon α secretion, in resting and stimulated cells from patients with systemic lupus erythematosus. Our findings highlight a groundbreaking immunoregulatory property of CXCR4 signaling that opens new therapeutic perspectives in inflammatory settings and autoimmune diseases.

INTRODUCTION

Type I interferons (IFNs) are key immune response mediators and, in humans, are composed of 13 IFN-α subtypes as well as IFN-β, IFN-ε, IFN-κ, and IFN-ω. Type I IFNs signal through a ubiquitously expressed common receptor (IFNAR) formed by two transmembrane proteins, IFNAR1 and IFNAR2. IFNAR engagement results in activation of the cytoplasmic kinases Janus kinase 1 (JAK1) and tyrosine kinase 2 (TYK2), leading to the formation of the transcription factor complex IFN-stimulated gene factor 3 (ISGF3). This complex translocates to the nucleus to promote transcription of IFN-stimulated genes (ISGs) (*1*). Type I IFNs exert antiproliferative and immunomodulatory effects, essential to control viral infection and spread. However, sustained overproduction of type I IFN can be deleterious for the host in various infection settings (*2*) and in a class of disorders collectively termed type I interferonopathies (*3*) composed of rare monogenic diseases and complex inflammatory/autoimmune diseases such as systemic lupus erythematosus (SLE).

The recurrent development of lupus-like symptoms in patients receiving recombinant type I IFN for treatment of hepatitis or hematological disorders highlights the frequent pathogenic effects of these molecules in individuals with susceptibility to autoimmune disorders. SLE is a heterogeneous disease at the clinical and molecular level, with at least seven subtypes identified by blood transcriptome profile in pediatric SLE (*4*). However, all subtypes present the common feature of increased IFN signaling. Moreover, we previously demonstrated that increased IFN-α levels in the serum of patients with SLE correlate with both disease activity [SLE disease activity index (SLEDAI)] and the expression of prognostic markers such as anti–double-stranded DNA (dsDNA) antibodies and complement activity (*5*).

Plasmacytoid dendritic cells (pDCs) are specialized in rapid and massive secretion of type I IFN (*6*–*8*). pDCs are activated after recognition of pathogen nucleic acids by sensors such as Toll-like receptors (TLRs). pDCs express TLR7 and TLR9 (*9*, *10*), which respond to single-stranded RNA (ssRNA) and imidazoquinolines (R848) (*11*, *12*) or DNA and CpG-containing oligonucleotides (*13*), respectively. TLR activation triggers production of type I IFN and proinflammatory cytokines through MyD88-mediated IRF7 signaling (*14*). Many studies have highlighted a central implication of pDCs in the development of SLE, making these cells paramount targets for innovative therapies (*15*). This is further supported by an up-regulation of TLR7-mediated IFN-α production by pDCs in patients with SLE (*16*). Despite evaluations of multiple therapeutic strategies including

[1]CNRS UMR-8601, CICB, 45 rue des Saints-Pères, 75006 Paris, France. [2]Team Chemistry & Biology, Modeling & Immunology for Therapy, CBMIT, Paris, France. [3]Université Paris Descartes, Sorbonne Paris Cité, Paris, France. [4]Institute of Molecular Virology, Ulm University Medical Center, Ulm 89081, Germany. [5]Immunobiology of Dendritic Cells, Institut Pasteur, Paris, France. [6]INSERM U1223, Paris, France. [7]Computational Biochemistry and Center of Medical Biotechnology, University of Duisburg-Essen, 45141 Essen, Germany. [8]Institute for Epidemiology and Medical Biometry, Ulm University, Ulm, Germany. [9]Imagine Institute, Paris, France. [10]Paediatric Haematology-Immunology and Rheumatology Department, Hôpital Universitaire Necker, Assistance Publique-Hôpitaux de Paris, Paris, France. [11]INSERM UMR 1163, Laboratory of Immunogenetics of Paediatric Autoimmunity, Paris, France. [12]Department of Paediatric Dermatology, Reference Centre for Rare Skin Disorders (MAGEC), Hôpital Universitaire Necker-Enfants Malades, Assistance Publique-Hôpitaux de Paris, 75015 Paris, France. [13]Hôpital Universitaire Robert Debré, Néphrologie pédiatrique, Paris, France. [14]CNRS UPR 3572 "Immunopathology and Therapeutic Chemistry"/Laboratory of Excellence Médalis, Institute of Molecular and Cellular Biology (IBMC), Strasbourg, France. [15]Department of Clinical Immunology and Internal Medicine, National Reference Center for Rare Autoimmune Diseases, University Hospital, Strasbourg, France. [16]UFR Medicine, University of Strasbourg, Strasbourg, France. [17]Centre for Translational Research, Institut Pasteur, Paris, France. [18]Pediatric Otolaryngology Department, Hôpital Necker-Enfants Malades, Assistance Publique Hôpitaux de Paris, Paris, France. [19]Institute of Transfusion Medicine and Immunogenetics (IKT) Ulm, Helmholtzstr. 10, 89081 Ulm, Germany. [20]INSERM U1016, Institut Cochin, Paris, France. [21]CNRS UMR 8104, Paris, France. [22]IRIM, Université de Montpellier, CNRS UMR, 9004 Montpellier, France.
*Corresponding author. Email: jean-philippe.herbeuval@parisdescartes.fr (J.-P.H.); nikaiafjsmith@gmail.com (N.S.)

anti-IFN and anti-IFNAR antibodies, a drug specifically targeting the type I IFN pathway in SLE fails to demonstrate efficacy. Molecular heterogeneity of SLE may provide an explanation for the failure of clinical trials based only on clinical diagnosis (*1*).

Previous studies have proposed the chemokine receptor CXCR4 as a promising drug target to reduce SLE symptoms in severe pathology through inhibition of inflammatory cell recruitment (*17*, *18*). Consistently, we recently discovered that binding of small natural and synthetic amino compounds to CXCR4 drives a profound immunosuppressive signaling in human pDCs (*19*). However, none of these amino compounds were highly specific for CXCR4. Therefore, we aimed to assess two specific ligands with high affinity for CXCR4: the small amino compound named IT1t that was identified as a potential candidate as it is the only small molecule that cocrystalized with CXCR4 (*20*) and the AMD3100 (Plerixafor), a Food and Drug Administration (FDA)–approved CXCR4 blocker used for $CD34^+$ bone marrow–derived progenitor cell collection before hematopoietic stem cell transplantation (*21*). IT1t and AMD3100 bind differently to CXCR4 into the major or the minor subpocket of CXCR4, respectively (*20*, *22*), which are also different from CXCL12 (CXCR4 natural ligand) binding sites.

We examined the effects of IT1t and AMD3100 on pDC activation and IFN production. Notably, we found that IT1t, but not AMD3100, strongly inhibits TLR7–type I IFN signaling in human pDCs from blood and tonsils. Moreover, IT1t controls inflammation in cells of patients with lupus and drastically reduced inflammation and levels of dsDNA antibodies, a pathogenesis marker, in a pristane-induced SLE mouse model. Our study identifies the IT1t binding site on CXCR4 as a potential modulator of pDC activity and places this pocket as a promising novel therapeutic target in autoimmune diseases.

RESULTS

IT1t controls TLR7-mediated type I IFN signaling in human pDCs in a CXCR4-dependent manner

We previously demonstrated that engagement of CXCR4 by natural amines and the synthetic mimic of histamine (clobenpropit) strongly inhibits viral-induced inflammation of human primary pDCs (*19*). To identify synthetic compounds with similar properties, we searched for known CXCR4 ligands with similar structures. The first cocrystalized structure of CXCR4 was achieved with a small compound called IT1t showing a strong structural homology with clobenpropit (fig. S1, A to C) (*20*). IT1t binds to an allosteric deep pocket that appears to be distinct from the FDA-approved CXCR4 antagonist AMD3100 binding site (fig. S1, D and E) (*23*, *24*). These pockets were called major pocket for the AMD3100 binding site (fig. S1F) and minor subpocket for the IT1t binding site (fig. S1G) (*20*, *22*), opening the possibility for distinct biological activity. Furthermore, IT1t K_i was evaluated previously and had a value of 0.41 ± 0.07 nM (*19*).

Given the central role of TLR7-driven type I IFN production in the pathophysiology of SLE, we investigated the ability of IT1t to control secretion of type I IFN by pDCs activated by distinct TLR7 agonists (R848 and HIV-1). A dose range from 0 to 50 μM AMD3100 and IT1t was added to pDCs in vitro in the presence or absence of R848 overnight. We first tested the potential cytotoxicity of both molecules on purified human pDCs (fig. S1H) activated by the TLR7/TLR8 synthetic stimulator R848 by flow cytometry and showed that neither IT1t nor AMD3100 induced toxicity up to 50 μM (fig. S1, I to M). R848 induced a massive increase of intracellular IFN-α production in purified pDCs (Fig. 1A). This increase was blocked in a dose-dependent manner by IT1t starting from 5 μM. In contrast, AMD3100 did not display any inhibitory activity as we previously reported (*19*). To verify the efficacy of AMD3100, we tested it on HIV-1 infection, and we confirmed that both AMD3100 and IT1t were able to block HIV-1 X4 tropism infection but not HIV-1 R5 tropism as previously demonstrated (fig. S1, N and O) (*25*, *26*). IT1t-specific inhibition of R848-induced IFN-α production in pDCs was confirmed with cells derived from six individual donors (Fig. 1, B and C). In agreement with a reduced intracellular expression of IFN, IT1t treatment also resulted in greatly reduced IFN-α/β protein concentrations in supernatants of R848-stimulated pDCs (Fig. 1D). To confirm the ability of IT1t to control TLR7-induced IFN-α, we evaluated its efficacy after HIV-1 stimulation, also known to be a strong TLR7 activator (*12*). As previously published (*19*), we did not observe any inhibitory activity of AMD3100. However, IT1t significantly reduced virus-induced IFN-α production at concentrations ≥5 μM (fig. S2, A to E). To further address the mechanism associated with IT1t inhibition of type I IFN in primary pDCs, we performed intracellular IFN-α and pIRF7 staining on R848-stimulated cells in the presence or absence of IT1t (Fig. 1, E and F). As expected, R848 treatment is associated with a strong increase of $pIRF7^+$ pDCs. Furthermore, 50% of the $pIRF7^+$ cells coexpressed IFN-α. Under IT1t treatment, pDCs failed to phosphorylate IRF7 and, consequently, did not express IFN-α. Furthermore, we showed by confocal microscopy that pIRF7 translocates into the nucleus of cells upon R848 activation (Fig. 1G), which was in turn inhibited by IT1t treatment (Fig. 1H). We validated the latest results by real-time quantitative polymerase chain reaction (RT-qPCR) and showed reduced levels of total IRF7 messenger RNA (mRNA) (Fig. 1G).

To definitively demonstrate that the IT1t immunoregulatory effect is dependent on CXCR4, we silenced CXCR4 expression using a previously established small interfering RNA (siRNA) protocol in human pDCs (*27*). We first confirmed the efficiency of our silencing by measuring CXCR4 mRNA expression by RT-qPCR (Fig. S3A). TLR7 stimulation by HIV particles strongly induced type I IFN and ISG (TRAIL or TNF-related apoptosis-inducing ligand) transcriptions, which were potently inhibited by IT1t. As expected, IT1t inhibitory effect on TLR7-mediated type I IFN and ISG transcription was almost abrogated in siCXCR4 but not in control siRNA cyclophilin B (siCTR)–treated cells (fig. S3, B and C).

To obtain more comprehensive insights into the effect of IT1t on pDC activation, we performed a gene expression array of 579 inflammatory markers in R848-stimulated pDCs from three donors treated or not with IT1t. Principal components analysis (PCA) showed that cells from each donor clustered together depending on treatment (Fig. 2A). Of the 579 genes analyzed, 136 significantly increased (n = 68) or decreased (n = 70) under R848 stimulation (Fig. 2B). Expectedly, 53% of the 68 genes up-regulated are IFN genes (n = 3) and ISGs (n = 32) (Fig. 2C). In comparison, pDCs stimulated with R848 and treated with IT1t display significant up-regulation of merely 18 genes (8 ISGs, 10 IFN). We further confirmed our results on selected genes by RT-qPCR on two different donors and showed that type I IFN, TRAIL, and MxA were inhibited in R848-stimulated pDCs by IT1t (Fig. 2D). Note that genes up-regulated by R848 treatment do not reflect the proportion of the different class of genes in the array. Notably, ISGs increased from 24% in the whole array to 48% in the R848-induced gene list, supporting the impact of this stimulation on type I IFN signaling (fig. S4).

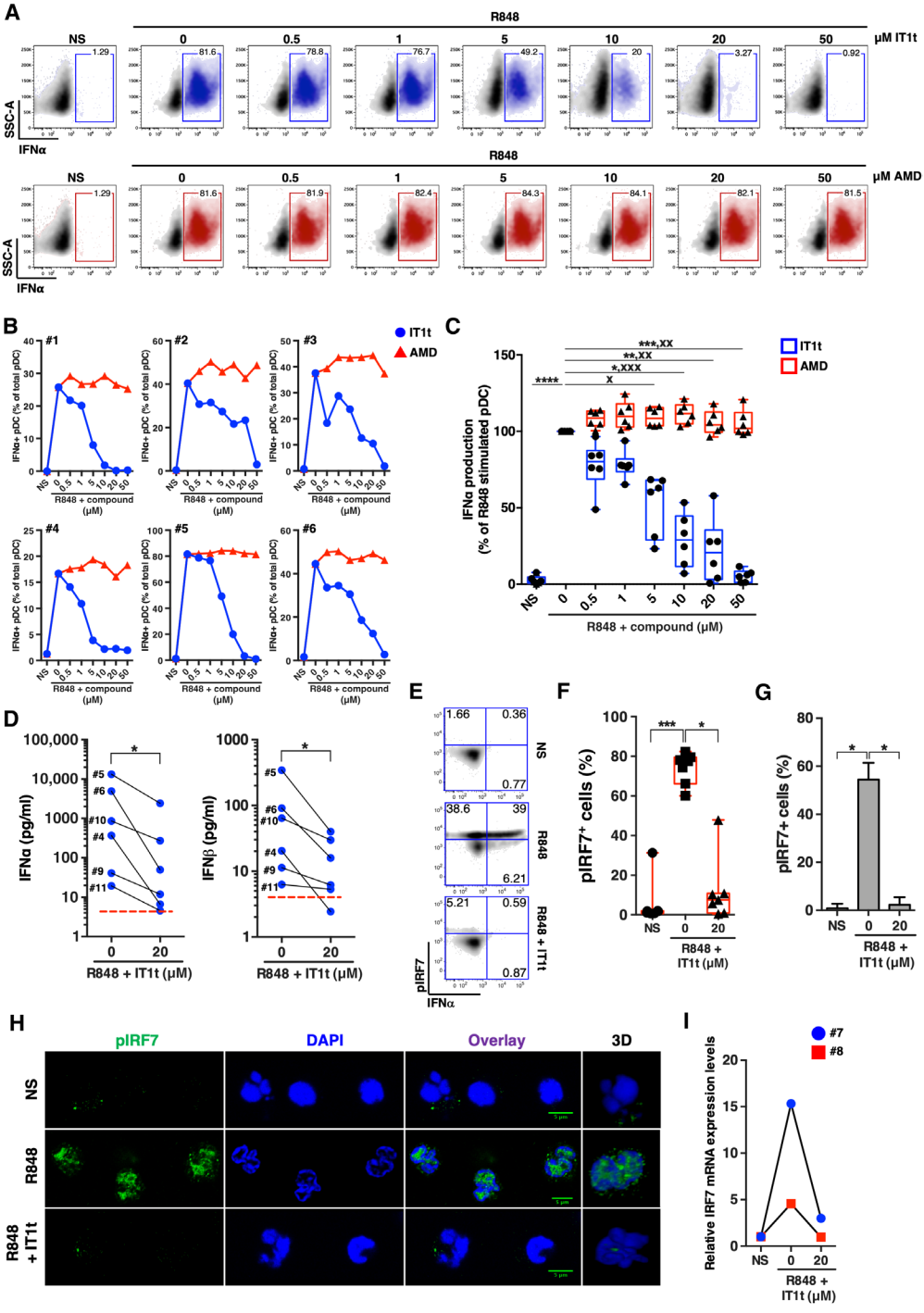

Fig. 1. IT1t suppresses TLR7-mediated IFN-α production in pDCs. Isolated human pDCs were preincubated with IT1t or AMD3100 and then stimulated with R848 overnight (5 μg/ml). (**A**) pDCs were cultured with R848 in the presence of increased dose of AMD3100 or IT1t. Intracellular levels of IFN-α were evaluated by flow cytometry. SSC-A, side scatter. (**B**) Individual and (**C**) combined representation of the effect of AMD3100 and IT1t on the IFN-α production of R848-stimulated pDCs from six healthy donors. Box and whisker plots with median ± minimum to maximum. Friedman test with Dunn's post hoc correction. "*" represents the statistical analysis comparing IT1t to the control R848 alone. "X" represents the statistical analysis comparing each concentration of IT1t to AMD3100. (**D**) Cytokine production was measured in the supernatant of the cells from six healthy donors using the multiplex bead-based immunoassay LEGENDplex. Average baseline of the nonstimulated condition is represented by the red dashed line. Wilcoxon test. (**E**) Intracellular levels of phosphorylated IRF7 and IFN-α were evaluated by flow cytometry. (**F**) Quantification of pIRF7 from seven individuals obtained by flow cytometry. Box and whisker plots with median ± minimum to maximum. Kruskal-Wallis with Dunn's post hoc correction. (**G**) Quantification by microscopy of the number of pIRF7^{+} pDCs out of 130 cells per condition in average. Friedman test with Dunn's post hoc correction. (**H**) Confocal microscopy of purified pDCs showing pIRF7 (green) and nucleus [DAPI (4′,6-diamidino-2-phenylindole), blue]. Scale bars, 5 μm. 3D was reconstructed with ImageJ using, on average, 30 stacks. (**I**) mRNA levels of IRF7 were quantified by RT-qPCR. ****$P < 0.0001$, ***$P < 0.001$, **$P < 0.01$, *$P < 0.05$. NS, nonstimulated.

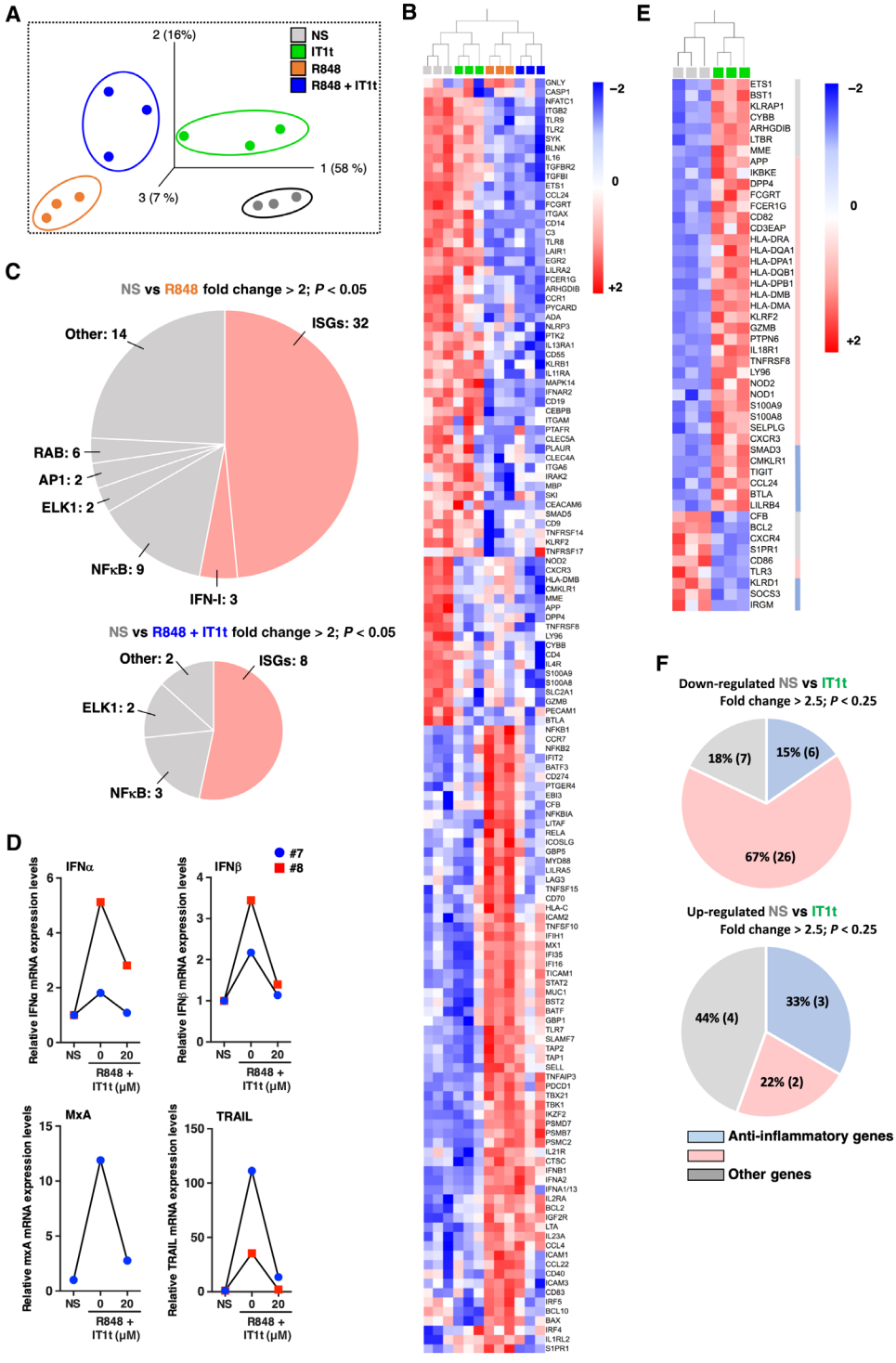

Fig. 2. IT1t prevents TLR7-mediated inflammation in pDCs. Isolated human pDCs were cultured with R848 (5 μg/ml) in the presence or absence of IT1t (20 μM). Total RNA from the cells was isolated and analyzed using the NanoString nCounter. (**A**) PCA was performed on the basis of 136 genes from the array differentially expressed between the NS (gray) and the R848 (orange) conditions. ($P < 0.05$, fold change > 2). (**B**) Heat map represents mRNA fold increase of the 136 genes significantly differently expressed between the NS and the R848 condition ($P < 0.05$, fold change > 2). (**C**) Pie chart representation of the promoters associated with genes significantly up-regulated between the NS and the stimulated (R848) condition and between the NS and the R848 + IT1t condition ($P < 0.05$, fold change > 2). The red parts represent ISGs (ISGF3 promoter) and the type I IFN (IRF7 promoter). Areas of the pie slices are representative of the number of genes. (**D**) mRNA levels of various genes were quantified by RT-qPCR for confirmation in two healthy donors. (**E**) Heat map represents the mRNA fold increase of 85 genes differently expressed between the NS (gray) and the IT1t (green) condition ($P < 0.05$, fold change > 2.5). (**F**) Pie chart represents the impact on inflammation of differently expressed genes between NS and IT1t. NS, nonstimulated.

The comparison of gene expression levels between the nonstimulated and the IT1t groups reveals that IT1t modulates gene transcription in the absence of stimulation (Fig. 2E). We identified 23 up-regulated and 62 down-regulated genes in pDCs treated with IT1t compared to the nonstimulated condition (fold change > 2.5; $P < 0.05$). IT1t treatment alone induced an enrichment of proinflammatory genes in the most down-regulated genes and an enrichment of anti-inflammatory genes, including SOCS1, SOCS3, and IRF4 in the most up-regulated genes (Fig. 2F). Together, these results demonstrate that IT1t treatment controls TLR7-induced type I IFN signaling in human pDCs at the transcriptomic and proteomic level in a CXCR4-dependent manner.

IT1t controls TLR7-mediated type I IFN and inflammation in mixed cell populations

As pDCs represent a very small fraction of immune cells in circulation (0.1 to 0.8%), we aimed to address whether we could target this rare population in the peripheral blood mononuclear cells (PBMCs). First, we assessed which leukocyte subsets in PBMCs could produce IFN-α upon R848 stimulation. R848 did not induce IFN-α production in $CD3^+$ T cells, $CD56^+$ NK (natural killer) cells, $CD3^+CD56^+$ NK T cells, $CD19^+$ B cells, or $CD14^+$ monocytes (Fig. 3A). However, a strong increase of IFN-α^+ pDCs was observed after stimulation. Overall, more than 90% of the IFN-α–producing cells were $CD123^+BDCA4^+$ pDCs (Fig. 3, B and C). Furthermore, treatment of PBMCs with IT1t reduced IFN-α production by pDCs in a dose-dependent manner (Fig. 3, D and E).

Human tonsils represent an integrative and physiological ex vivo model to study innate immune responses at the mucosal interface (Fig. 4A) (*28*, *29*). We thus tested IT1t biological activity on tonsil mononuclear cell suspensions (TMCs), which mimic the role of a secondary lymphoid organ. We first characterized the immune profile of cells present in the culture and quantified the number of pDCs, which represents about 5% of the lineage-negative HLA-DR–positive (Lin^-DR^+) immune cells (Fig. 4, B and C). Stimulation of TMCs overnight with R848 increased the frequency of IFN-α^+ pDCs about 10-fold, and treatment with IT1t (20 μM) resulted in a 67% reduction of this induction (Fig. 4D). We thus took advantage of the cellular diversity of the TMC model to evaluate the impact of IT1t on a broader set of inflammatory molecules. TMCs from seven donors were stimulated with R848 in the presence or absence of IT1t. IT1t reduced type I and type II IFN, proinflammatory cytokines [IL-6 (interleukin-6), TNF-α (tumor necrosis factor–α), IL-1β, IL-12p70, and GM-CSF (granulocyte-macrophage colony-stimulating factor)],

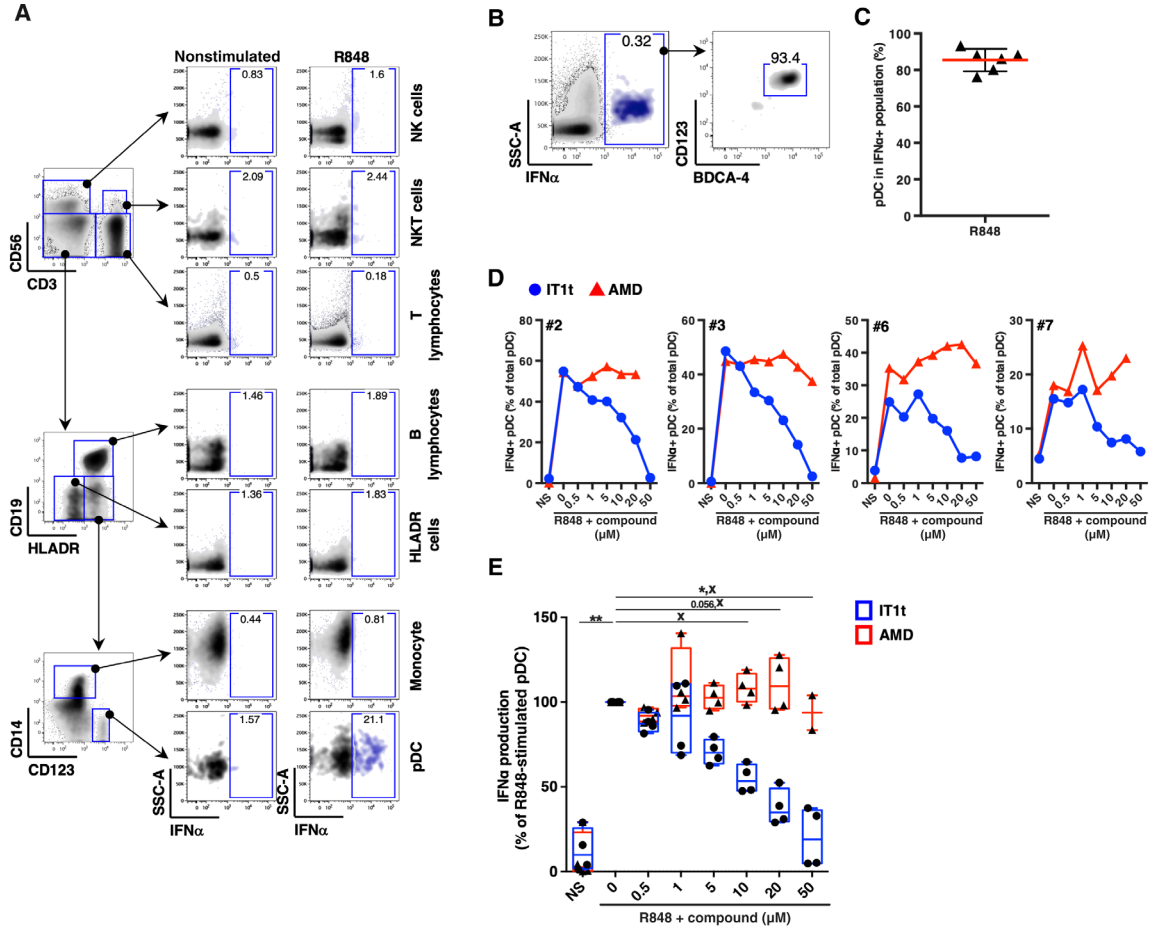

Fig. 3. IT1t blocks TLR7-mediated IFN production of circulating pDCs in PBMC cultures. (**A** and **B**) PBMCs from healthy individuals were cultured with R848 (5 μg/ml). IFN-producing cells were identified by flow cytometry. (**C**) Percentage of pDCs within the IFN-α^+ PBMCs after R848 stimulation from six different donors. (**D**) Individual and (**E**) combined representation of the effects of AMD3100 and IT1t on R848-induced IFN-α production in the pDC fraction from PBMCs from four healthy donors. Box and whisker plots with median ± minimum to maximum. Friedman test with Dunn's post hoc correction. "*" represents the statistical analysis comparing IT1t to the control R848 alone. "X" represents the statistical analysis comparing each concentration of IT1t to AMD3100. $^{**}P < 0.01$, $^{*}P < 0.05$. NS, nonstimulated.

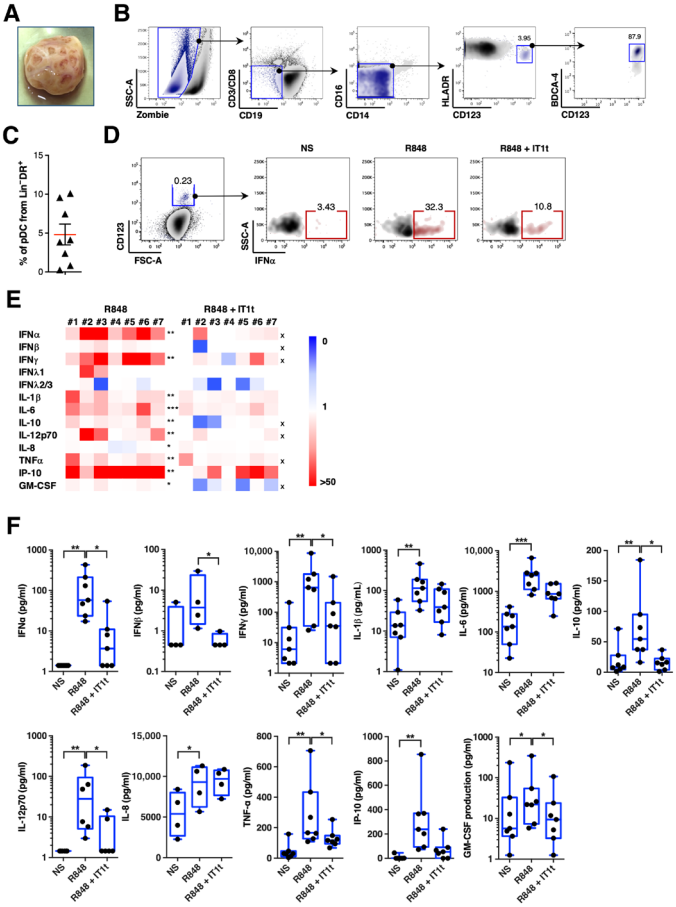

Fig. 4. IT1t suppresses TLR7-mediated inflammation in tonsil resident pDCs. (**A**) Picture of human tonsil after surgical removal. (**B**) pDCs from tonsils were identified as CD8-CD3-CD16-CD14-CD123 + HLADR$^+$BDCA-4$^+$. (**C**) Percentage of pDCs within the Lin$^-$DR$^+$ cells from eight human tonsils. (**D**) TMCs of healthy individuals were cultured with R848 (5 μg/ml) in the presence or absence of IT1t (20 μM). IFN$^+$ pDCs were identified and quantified by flow cytometry. (**E** and **F**) Effect of IT1t on R848-stimualted TMCs was evaluated in the supernatant of seven healthy individuals using LEGENDplex. (E) Heat map represents the fold increase in cytokine secretion compared to NS. "*" represents the statistical analysis comparing the R848 to the NS condition. "X" represents the statistical analysis comparing the R848 to the R848 + IT1t condition. (F) Graphs represent the concentration in picograms per milliliter of each measured cytokine. Box and whisker plots with median ± minimum to maximum. Friedman test with Dunn's post hoc correction. *** or $^{XXX}P < 0.001$, ** or $^{XX}P < 0.01$, * or $^{X}P < 0.05$. (Photo credit: N. Smith, CNRS UMR-8601, CBMIT, Université Paris Descartes, Paris, France, and Institute of Molecular Virology, Ulm University Medical Center, Ulm, Germany.) NS, nonstimulated.

and chemokine (CXCL-10) protein production in cells from all seven donors (Fig. 4, E and F). Therefore, IT1t controls type I IFN and a large spectrum of inflammatory cytokine production in isolated pDCs, as well as in complex cell populations.

IT1t suppresses inflammation and disease progression in an SLE mouse model

We next aimed to evaluate whether IT1t-mediated immune modulation could have an impact in inflammatory disease progression. SLE represents one of the most common interferonopathies (*30*). TLR7 and TLR7-mediated IFN signaling are well documented as a major player of SLE disease development (*16*, *31*–*33*) and response to treatment (*34*). Several mouse models have led to a clearer understanding of the role of type I IFN in the pathogenesis of lupus-like disease. Nevertheless, pristane-induced SLE meets most of the Systemic Lupus Erythematosus International Collaborating Clinics (SLICC) criteria used for human lupus classification, with the presence of an IFN signature and anti-dsDNA antibodies (*35*). Pristane induces type I IFN production mainly through the TLR7/MyD88 pathway (*36*). TLR7 deficiency not only abolishes pristane-induced type I IFN production but also prevents autoantibody production and renal disease, indicating a key role of TLR7/MyD88/type I IFN pathway in this model (*36*, *37*). Given the broad immunoregulatory properties of IT1t under TRL7 stimulation, including inhibition of type I and type III IFNs, TNF-α, and IL-6 protein production, we evaluated the effect of IT1t as a valuable therapeutic approach for SLE.

First, by using either a system of reporter cell line measuring all types of IFN (STING-37 cells) (*38*) or a specific IFN-α bead assay (LEGENDplex), we showed that in ex vivo tonsil cultures, pristane induced IFN-α production, which was significantly reduced by IT1t treatment (Fig. 5, A and B). Then, SLE was induced in BALB/c mice by daily intraperitoneal coinjection of pristane (0.5 ml per mouse) with vehicle or with different IT1t doses (3, 10, and 30 mg/kg or mpK) for 10 weeks. As a reference treatment, SLE mice were treated daily with the corticosteroid prednisolone at 15 mpK (Fig. 5C). IT1t-treated mice did not demonstrate any sign of stress or weight loss as compared to vehicle, indicating the good tolerance of the treatment by the animals (Fig. 5D).

Cytokines IFN-α, IL-1β, IL-17, TNF-α, and TRAIL were quantified as markers for SLE from serum at weeks 4 and 10. It should be noted that IFN-α was not detectable in serum of pristane-treated mice. However, we could detect increased levels of the IFN-induced protein TRAIL and of inflammatory cytokines. Prednisolone treatment was used as a positive therapeutic control and reduced all cytokines measured (Fig. 5, E to H). IT1t, similarly to prednisolone, strongly reduced production of IL-1β, IL-17, and TRAIL in a dose-dependent manner (Fig. 5, E to H). The production of TNF-α at week 10 was totally inhibited by prednisolone in contrast to IT1t treatments (Fig. 5G). Thus, these results suggest a distinct pattern of immunosuppressive activity of prednisolone and IT1t in SLE mice. The severity of SLE pathogenesis was also estimated by measuring levels of dsDNA antibodies. The high dose of IT1t significantly decreased anti-dsDNA levels during the whole treatment as early as week 4, in contrast to prednisolone, which only significantly reduced antibodies levels at week 8 (Fig. 5I). In line with this observation, we observed a reduced proportion of mice developing glomerulonephritis in the groups treated with 10 and 30 mpK of IT1t compared to vehicle (Fig. 5J). Together, these results highlight that intraperitoneal injection of IT1t reduces SLE-associated phenotypes faster than the reference corticosteroid treatment and with a greater selectivity on cytokine production.

IT1t controls type I IFN in vitro in cells from patients with SLE

SLE is a chronic disease characterized by periods of low disease activity and periods of high disease activity termed "flares," where patients experience an inflammatory storm associated with fever and skin rash (*39*). We recently demonstrated that circulating levels of IFN-α are higher in SLE patients with greater disease activity (*5*). Therefore, we evaluated whether IT1t treatment reduces TLR7-mediated IFN-α production in these patients. PBMCs from healthy controls and patients with lupus were stimulated with R848 to mimic an inflammatory burst with a strong type I IFN signature (Fig. 6A).

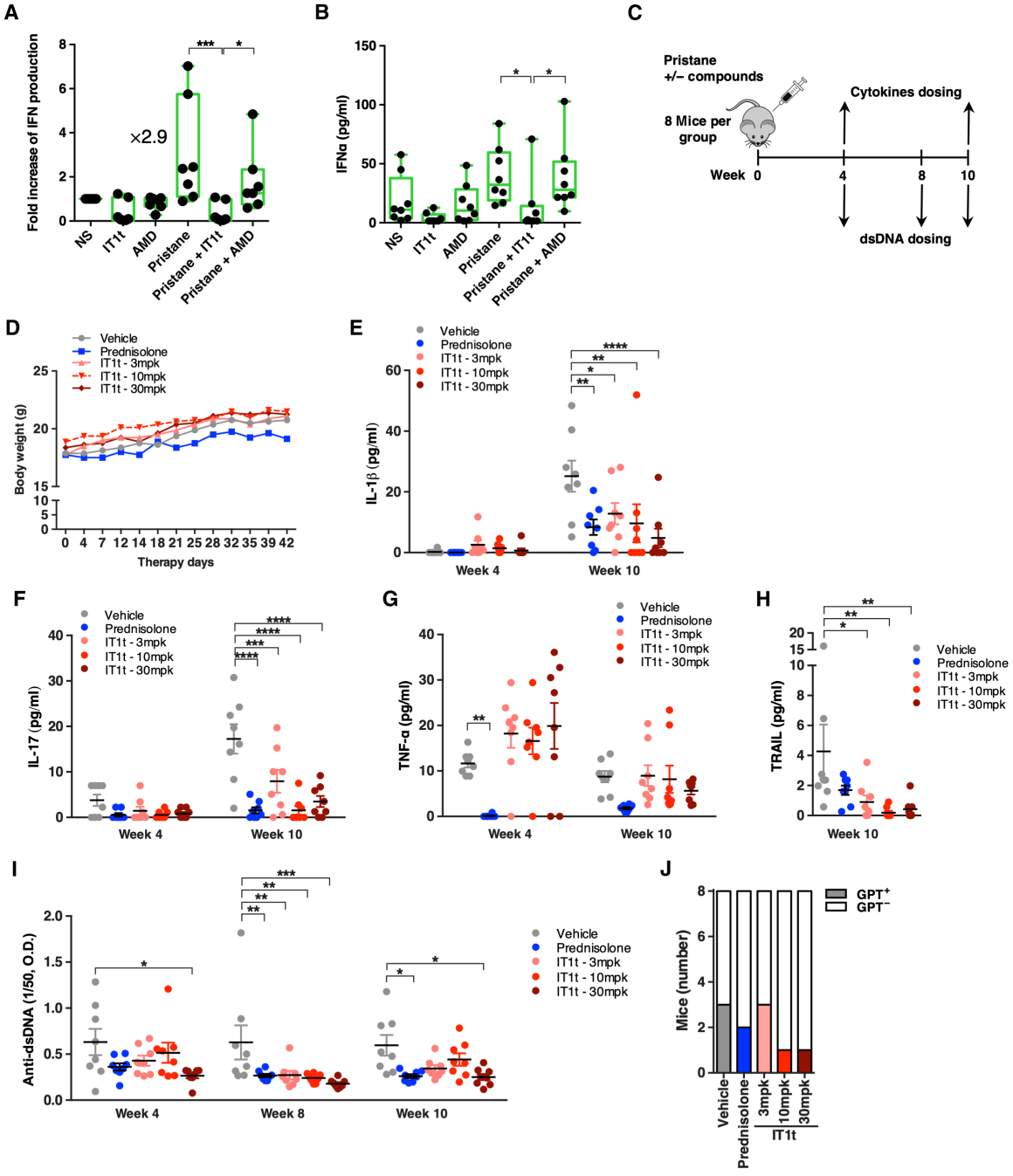

Fig. 5. IT1t reduces TLR7-mediated inflammation and markers of disease progression in SLE mice. Human TMCs were preincubated with IT1t or AMD3100 (20 μM) and stimulated overnight with pristane (200 μg/ml). IFN production was measured in supernatants using (**A**) the STING-37 reporter cell line or (**B**) the multiplex bead-based immunoassay LEGENDplex. Box and whisker plots with median ± minimum to maximum. Kruskal-Wallis test with Dunn's post hoc correction. (**C**) Mice were injected intraperitoneally daily with 0.5 ml of pristane to induce disease and with treatment consisting of prednisolone (15 mg/kg) or 3, 10, or 30 mpK of IT1t for 10 weeks. (**D**) Body weight was measured. (**E** to **H**) Inflammatory status was evaluated in the serum of mice by protein dosage of IL-1β (E), IL-17 (F), TNF-α (G), and TRAIL (H). Two-way repeated-measures analysis of variance (RM ANOVA) with Bonferroni post hoc correction. One-way ANOVA for TRAIL. (**I**) Anti-dsDNA antibody titers were measured on weeks 4, 8, and 10. Two-way RM ANOVA with Bonferroni post hoc correction. (**J**) Relative proportion of mice that develop glomerulonephritis in each group compared to the vehicle was assessed. All data are presented as mean ± SEM. ****$P < 0.0001$, ***$P < 0.001$, **$P < 0.01$, *$P < 0.05$. $n = 8$ mice per group. NS, nonstimulated.

IT1t treatment controlled IFN production in patients' and controls' PBMCs (Fig. 6B). Intracellular flow cytometry analysis reveals that R848-induced IFN production by patient and control PBMCs was mainly restricted to pDCs, which is in line with our previous observations. Furthermore, this IFN production by pDCs was abrogated by IT1t treatment (Fig. 6, C and D).

In humans, SLE is known to be a very heterogeneous disease with a large phenotypic and inflammatory spectrum (*40*). This heterogeneity

was observed in cultured PBMCs from patients, with some demonstrating a measurable spontaneous inflammation (SpI patients), while being undetectable in others. To assess the capacity of IT1t to control human lupus–driven spontaneous inflammation, we cultured PBMCs of four patients and monitored IFN-α secretion by digital ELISA (enzyme-linked immunosorbent assay), STAT1 (signal transducer and activator of transcription 1) and STAT3 phosphorylation status by flow cytometry, and inflammatory transcript levels by RT-PCR (Fig. 6E). For all patients with constitutive in vitro secretion of IFN-α, we observed a strong inhibition with IT1t treatment (Fig. 6F). Similarly, in cells from patients with spontaneous up-regulation of pSTAT1 and pSTAT3, IT1t treatment was associated with a reduction of STAT1 and STAT3 phosphorylation to a level similar to cells from healthy individuals (Fig. 6, G to J). Despite heterogeneous inflammatory profiles, treatment with IT1t consistently normalized the level of inflammatory gene transcripts in cells from patients with lupus (Fig. 6K), suggesting that targeting of CXCR4 by IT1t constitutes a promising strategy for controlling human inflammation.

DISCUSSION

New strategies to block the type I IFN pathway in SLE pathology are of great interest. In this study, we show that IT1t, a CXCR4 minor pocket ligand, has a strong immunosuppressive activity on TLR7-activated pDCs. Furthermore, IT1t treatment controlled inflammation, reduced dsDNA antibody titers in a lupus mouse model, and controlled type I IFN production and signaling in cells isolated from patients with lupus. We propose to consider targeting CXCR4 using small amino compounds such as IT1t as a potential innovative therapeutic strategy in interferonopathies.

pDCs are specialized in rapid and massive secretion of type I IFN in response to innate immune sensor stimulation from the TLR family (*8*, *10*, *41*, *42*). There is supporting evidence that overproduction of type I IFN by pDCs is central in development and progression of numerous inflammatory diseases (*43*, *44*). Thus, we aimed to specifically target pDC activation. We previously showed that clobenpropit (CB), an antihistamine, modulates pDC activation by engagement of CXCR4 (*19*). Therefore, as pDCs express high levels of CXCR4, we hypothesized that pDC activation could be specifically targeted with small amino compounds interacting with this chemokine receptor. However, given the large expression profile of histamine receptors, it is challenging to predict the mechanism of action in a mixed cell population or in a small animal model. We identified IT1t as a compound with similar immunoregulatory properties to histamine and with a high specificity toward CXCR4. We demonstrated that IT1t but not AMD3100, a clinically used CXCR4 antagonist, exhibits strong inhibitory activity on type I IFN production by TLR7-activated primary pDCs. Notably, both synthetic ligand (R848) and viral (HIV) activation of pDCs were strongly inhibited by IT1t but not by AMD3100. This raises the ability of amino compounds targeting CXCR4 to be considered as therapeutic strategies in both inflammatory and chronic infectious diseases, where sustained production of type I IFN is thought to impair the immune response (*45*–*47*).

It is clear that IT1t inhibitory activity on isolated primary pDCs was fully dependent on CXCR4 engagement as demonstrated by the loss of the IT1t effect in CXCR4 siRNA-treated cells. The IFN-α produced following R848 stimulation in human TMCs and PBMCs from healthy controls and patients with SLE was mostly due to pDCs. Together, our in vitro data validate IT1t as a potent inhibitor of type I IFN production by activated pDCs.

Targeting type I IFN production and proinflammatory cytokines in chronic diseases is the predominant therapeutic option in SLE (*48*). However, despite the identification of the up-regulation of IFN signaling in SLE decades ago (*49*, *50*), anti-IFN therapies have developed slowly owing to the heterogeneity of SLE disease progression (*48*) and have yet to reach routine clinical practice. Antibody-based IFN therapies have not yet progressed beyond phase 2 development, while the more promising anti-IFNAR approach (*51*) recently failed to achieve the primary end point in a phase 3 clinical study. Specific targeting of pDCs has provided promising results (*52*), leading to clinical trials based on anti-BDCA2 and anti-CD123 antibodies in phase 2 and phase 1 trials, respectively (*51*). Small molecule–based approaches to control IFN in SLE remain largely unexplored. TBK1 inhibition has demonstrated promising results in mice (*53*), but no inhibitor of IFN secretion has yet entered clinical trials. An alternative strategy that consists of blocking IFNAR signaling with several JAK2 inhibitors is currently evaluated in phase 2 clinical studies (*51*). In this context, we evaluated the effect of chronic IT1t intraperitoneal injection in an SLE pristane-induced mouse model. Several mouse models have led to a clearer understanding of the role of type I IFN in the pathogenesis of lupus-like disease. Pristane-induced SLE meets many SLE features including an IFN signature and anti-dsDNA and anti-RNA antibodies, and reaches a score of 8 in the SLE criteria (*35*). In pristane-induced murine lupus, TLR7 is specifically required for the production of RNA-reactive autoantibodies and the development of glomerulonephritis (*36*). TLR7 deficiency not only abolishes pristane-induced type I IFN production but also eliminates autoantibody production and renal disease, indicating a key role of the TLR7/MyD88/type I IFN pathway in this model (*35*, *54*, *55*). We demonstrate here that IT1t treatment by targeting the TLR7 pathway inhibits the systemic production of IL-1β, IL-17, and the IFN-induced protein TRAIL similarly to prednisolone in pristane-induced SLE mice. Furthermore, IT1t exhibited a better reduction of dsDNA antibodies, which serve as a diagnostic and prognostic marker, than prednisolone. To sum up, IT1t provides a new therapeutic alternative to corticosteroids for IFN-triggered SLE pathogenesis.

In view of the promising effect of IT1t in healthy donors and the SLE mouse model, we tested IT1t on cells isolated from patients with lupus. Patients with SLE experience periods of low disease activity and also periods of "flares," where they undergo an inflammatory storm (*39*). Flares are also associated with a massive increase in the IFN signature in patients' blood. To mimic "flares" in vitro, we stimulated patient's cells with R848. Using pan–IFN-α ultrasensitive digital ELISA (*5*), we demonstrate that IT1t treatment controls IFN-α secretion in activated PBMCs from patients with lupus, acting preferentially through diminution of IFN-α^+ pDCs. In our hands, spontaneous secretion of IFN-α by frozen PBMCs of adult patients with SLE is almost never detectable. However, using digital ELISA, we detected IFN secretion on several occasions from fresh ex vivo unstimulated cultures of PBMCs from juvenile SLE. We identified four patients with clear, albeit distinct, spontaneous inflammatory profiles. For all patients' cells, and irrespective of their specific inflammatory profile, IT1t treatment was associated with a reduction of IFN-α secretion, pSTAT1, and pSTAT3 levels, as well as ISG and cytokine transcription. These promising results with patients' cells, using a small CXCR4

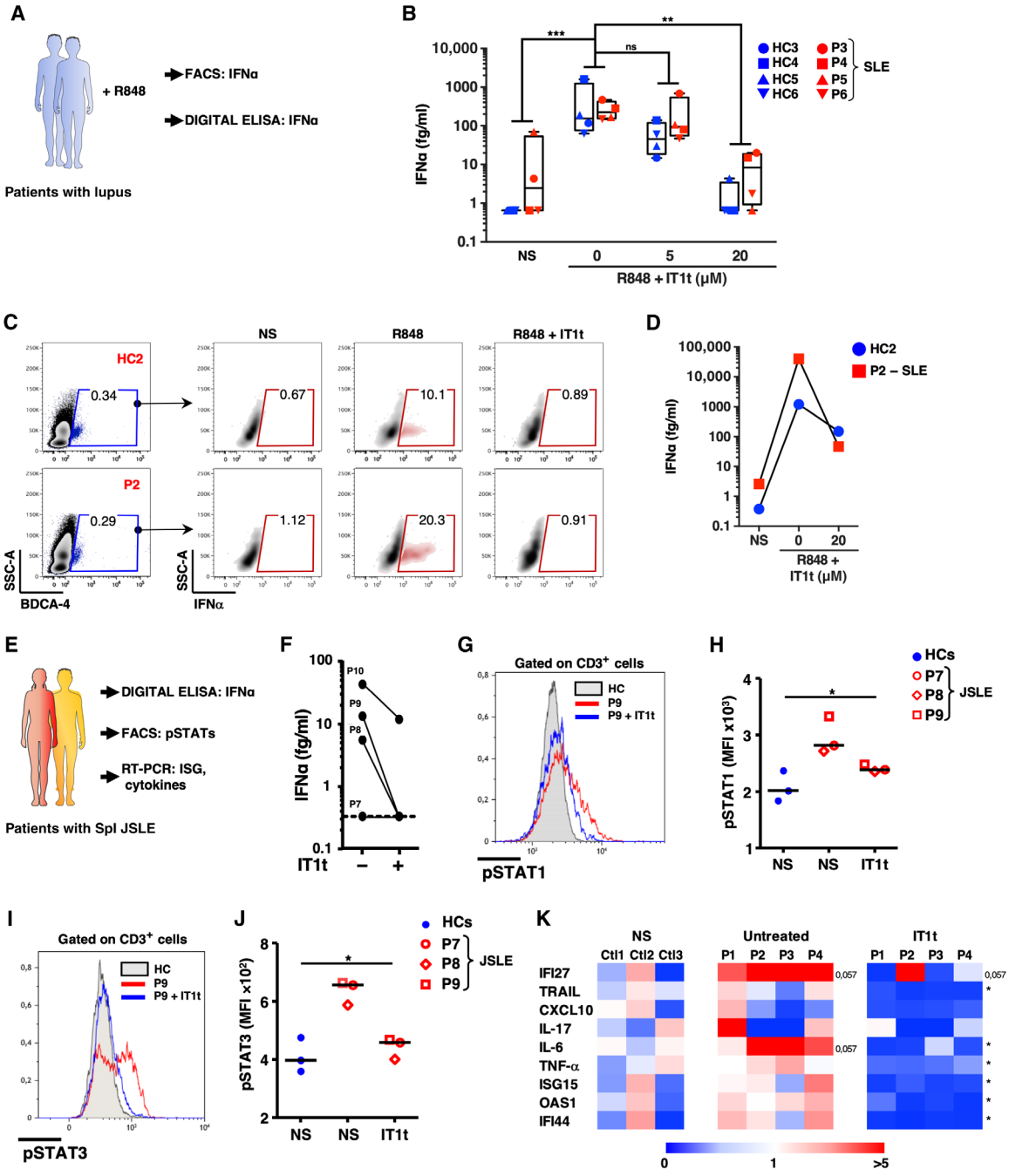

Fig. 6. IT1t controls induced and spontaneous inflammation in vitro in cells from patients with SLE. (**A**) PBMCs from healthy controls (HC) and patients with lupus (P) were stimulated with R848 to recapitulate disease flares and treated or not with IT1t (20 μM). Effect of IT1t was evaluated by IFN-α dosage in cell supernatants by digital ELISA (Simoa) or by intracellular IFN-α expression by flow cytometry. (**B**) Effect of IT1t on IFN-α secretion from TLR7-stimulated cells from patients (P3, P4, P5, and P6) was measured by Simoa. Box and whisker plots with median ± SEM showing minimum to maximum. Friedman test with Dunnett post hoc correction. (**C**) Intracellular IFN-α expression was assessed by flow cytometry and (**D**) IFN-α was dosed in the supernatant of cells from P1 stimulated with R848 (5 μg/ml) and treated with IT1t. (**E**) Effect of IT1t on cells from patients with spontaneous inflammation (SpI) juvenile SLE (JSLE) was evaluated on IFN-α production by (**F**) Simoa in the cell supernatant, by flow cytometry to measure pSTAT1 (**G** and **H**) and pSTAT3 (**I** and **J**), and by RT-qPCR (**K**) to quantify mRNA levels in PBMCs from four different patients with JSLE. (H and J) Friedman test. ***$P < 0.001$, **$P < 0.01$, *$P < 0.05$. NS, nonstimulated.

agonist with previously unappreciated immunoregulatory properties, open new perspectives for the treatment of lupus.

Numerous CXCR4 ligands have been described, including pyridines, quinolones, peptides, or polyazamacrocycle with a large range of affinities (*56*). The excellent control of TLR7-mediated pDCs inflammation by IT1t brings a new level of complexity to CXCR4 signaling and associated functions. Initially characterized by crystallography in 2010, the IT1t binding site has since been further studied. A

combination of structure- and ligand-based virtual screening of the "IT1t pocket" (*57*) identified a set of small molecules with agonist or antagonist properties toward CXCL12, demonstrating the functionality of this pocket. In a previous study, we demonstrated that another thiourea CXCR4 ligand (CB) showed similar biological inhibitory properties to IT1t in vivo (*19*). This highlights the complexity of CXCR4 engagement and validates the IT1t CXCR4 minor pocket as a promising pharmacological target for chronic diseases in contrast to the CXCR4 major pocket of AMD3100 (*20*, *23*). We acknowledge that we have not yet resolved the molecular mechanism linking CXCR4 engagement to TLR7 signaling inhibition. Furthermore, we also found that TLR4/TLR8/TLR9 response in pDCs and monocytes is also drastically inhibited by IT1t, suggesting a broader effect on immune modulation. Thus, understanding the molecular pathway will be the next step to fully characterize the role of CXCR4 in control of innate immunity. However, we can still speculate on some hypothesis. One could be that IT1t binding on CXCR4 blocks TLR pathway by affecting the intracellular vesicular trafficking (*58*). This hypothesis can be supported by the observation that chloroquine, which is known to impair many lysosomal functions, is also a strong inhibitor of IFN production by TLR-stimulated pDC and is used in the clinic to treat patients with lupus.

In conclusion, this study demonstrates that the CXCR4 cocrystalized ligand IT1t controls TLR7-mediated inflammation in human pDCs, controls inflammation and autoantibody formation in mice with lupus, and alleviates induced or spontaneous inflammation from cells of patients with SLE. Thus, IT1t and, by extension, the CXCR4 minor subpocket represent a novel promising axis for therapeutic options in chronic inflammation and autoimmune diseases.

METHODS

Study design

The aim of the study was to evaluate the effect of known antagonists (IT1t and AMD3100) of the chemokine receptor CXCR4 on the modulation of the innate immune response in pDCs and its potential usage as a new therapy in lupus. The sample sizes (healthy donors or patients with lupus) for this exploratory study were designed to ensure robust statistical results, while adhering to experimental feasibility and minimization of donors. Sample size for mice data was designed to maximize statistical power, whereas no randomization or blinding was implemented. Details on sampling and experimental replicates are provided in each figure legend.

Human samples

The study was approved by the Comité de Protection des Personnes (ID-RCB/EUDRACT: 2014-A01017-40) and AC-2014-2289. Investigations were undertaken with written informed consent.

Blood samples, isolation, and culture of blood leukocytes

The blood from healthy donors was obtained from two sources, either from "Etablissement Français du Sang" (convention # 07/CABANEL/106; Paris, France) or from the Apheresis and Blood Donation Unit at the Institute of Clinical Transfusion Medicine and Immunogenetics (Ulm, Germany), after being approved by the Institutional Review Board at Ulm University. For material of patients with lupus, the study was approved by the Comité de Protection des Personnes (ID-RCB/EUDRACT: 2014-A01017-40 and 2018-A01358-47) in France. Experimental procedures with human blood have been approved by the Necker Hospital Ethical Committees for human research and were done according to the European Union guidelines and the Declaration of Helsinki, and informed consent was obtained from all donors (healthy and patients). The clinical data of patients with lupus are summarized in table S1. In vitro experiments were performed using human PBMCs isolated by density centrifugation from peripheral blood leukocyte separation medium (Cambrex, Gaithersburg, MD). Human pDCs were purified by negative selection with the EasySep Human Plasmacytoid DC enrichment kit (STEMCELL Technologies). After purification, we obtained purity higher than 91% for pDCs quantified by flow cytometry. PBMCs and pDCs were cultured in RPMI 1640 (Invitrogen, Gaithersburg, MD) (R10) containing 10% heat-inactivated fetal bovine serum, penicillin (100 U/ml), streptomycin (100 μg/ml; 1% pen-strep), and 1 mM glutamine (HyClone, Logan, UT). Frozen PBMCs from controls and patients with lupus were cultured in RPMI 1640 (Invitrogen, Gaithersburg, MD) (R5) containing 5% heat-inactivated human serum AB (Sigma-Aldrich, MO, USA). The healthy donors were identified from #1 to #11 (Figs. 1 to 3) or HC3 to HC6 (Fig. 6) and P1 to P10 for patients with SLE and JSLE.

TMCs isolation from tonsils

Collection of tonsils was approved by the Comité de Protection des Personnes (ID-RCB/EUDRACT: 2018-A01358-47). Obstructive tonsils from healthy children with sleep apnea were removed after a partial tonsillectomy. The tissue was kept in phosphate-buffered saline (PBS) 1× no longer than 2 hours, cut into small pieces, and disrupted using a glass pestle onto a 60-mesh steel grid. The TMCs were filtered on a 70-μm filter and washed in PBS. Ficoll separation was further performed to remove the rest of the epithelial tissue and debris. TMCs were cultured in R10. The donors were identified from #1 to #7.

CXCR4 knockout experiments

pDCs were seeded at 10^5 cells/100 μl in 96-well plates and incubated at 37°C. Cyclophilin B (control) and CXCR4 siRNA (SMARTPool, Dharmarcon) were diluted in DOTAP (1,2-dioleoyl-3-trimethylammonium-propane; Roche Applied Sciences). The mix was gently mixed and incubated at room temperature for 15 min. After incubation, the mix was added to cells in culture at a final concentration of 160 nM. Last, cells were incubated at 37°C for 24 hours before adding the stimulation for 16 hours.

Cell stimulation

PBMCs and TMCs were seeded at 2×10^6/ml, and purified pDCs were seeded at 5×10^4/100 μl. Cells were then stimulated with the TLR7/TLR8 agonist Resiquimod (R848; Invivogen) at 5 μg/ml or inactivated AT-2 HIV-1_{MN} (X4 tropism) and HIV-1_{ADA} (R5 tropism) at 60 ng/ml $p24^{CA}$ equivalent [provided by J. D. Lifson (SAIC-NCI, Frederick, MD)] or pristane at 200 μg/ml (Sigma-Aldrich). Purified pDCs were pretreated with the IT1t (Tocris Bioscience) or AMD3100 (Sigma-Aldrich) at 20 μM (or other if specified for 1 hour before 16 hours of stimulation or as indicated). Cells were then collected for RT-qPCR, and supernatants were collected for cytokine detection. For intracellular IFN-α staining, brefeldin A was added to the cells at the same time as the stimulus. Cells were then collected and stained for flow cytometry analysis.

Cell infection

TZM-bl cells were seeded in flat-bottomed 96-well dishes, cultured overnight, and incubated with various concentrations of AMD3100

or IT1t for 1 hour before they were infected with virus containing 20 ng of p24 antigen in a total volume of 100 ml of medium. Three days after infection, the cells were lysed, and infection rates were determined using the one-step Tropix Gal-Screen Kit as recommended by the manufacturer.

Flow cytometry

Cells were washed in PBS and then incubated with a viability stain (Zombie-Aqua, BioLegend) for 30 min at 4°C. After washing, the cells were resuspended in PBS containing 2% fetal calf serum and 2 mM EDTA and stained with the extracellular mix using APC (allophycocyanin) anti-BDCA4 (clone 12C2), fluorescein isothiocyanate anti-CD123 (clone 6H6), PerCP.cy5.5 anti-CD56 (clone 5.1H11), BV421 anti-HLADR (human leukocyte antigen–DR isotype) (clone L243), PE.cy7 anti-CD19 (clone 4G7), and APC-cy.7 anti-CD14 (clone M5E2) all from BioLegend and used at 1:200 and V500 anti-CD3 (clone SP34-2, 1:200; BD Bioscience). For IFN-α intracellular staining, a Fixation/Permeabilization Solution Kit (BD Cytofix/Cytoperm) was used according to the manufacturer's protocol. Briefly, the cells were fixed for 10 min at 4°C with 100 μl of the Fixation/Permeabilization solution and then washed and stained in 100 μl of the BD Perm/Wash Buffer containing PE (phycoerythrin) anti–IFN-α (clone REA1013, 1:50; Miltenyi Biotec) antibody for 1 hour at 4°C. For pIRF7 staining, following the extracellular staining, the cells were fixed in 2% paraformaldehyde for 10 min at 4°C and then washed and permeabilized with 90% ice-cold methanol for 20 min at 4°C. The cells were stained with Alexa Fluor 488-IRF7 pS477/pS479 (K47-671, 1:25; BD Biosciences) and PE anti–IFN-α antibodies for 1 hour at 4°C. Data acquisition was performed on a FACSCanto II flow cytometer using FACSDiva software (BD Biosciences, San Jose, CA). FlowJo software (Treestar, Ashland, OR) was used to analyze data.

Confocal microscopy

Purified pDCs were pretreated or not with IT1t at 20 μM and then stimulated with R848 overnight, in the presence of brefeldin A. Cells were washed in ice-cold PBS–bovine serum albumin (BSA; 0.2%) and then were plated on poly-D-lysine–coated slides and fixed with 4% paraformaldehyde. Cells were permeabilized with 90% ice-cold methanol for 20 min at 4°C and, after washing, were incubated with Alexa Fluor 488–IRF7 pS477/pS479 antibody in 0.5% saturation buffer PBS-BSA. Last, slides were washed in PBS and mounted in Fluoromount-G with DAPI (4′,6-diamidino-2-phenylindole) medium (Thermo Fisher Scientific). Images were digitally acquired with a Zeiss LSM 710 confocal microscope using 63× PL APO O.N. 1.4 per oil objective. All analyses were performed using the ImageJ software (National Institutes of Health, Bethesda, MD, USA). The plugin 3D Viewer was used to create three-dimensional images.

All types of IFN detection

To quantify the secretion of functional IFN in TMCs, we used a biological assay based on a stable cell line where luciferase reporter gene is controlled by five IFN-stimulated response elements (STING37 cell line). First, TMCs supernatants were harvested after 24 hours of stimulation and frozen at −20°C for storage. Then, TMCs supernatants were dispensed in culture wells of a 96-well plate containing 35×10^3 STING37 cells per well. After 24 hours of culture, luciferase activity was determined by adding 50 μl of Bright-Glo reagents (Promega) to culture wells and measuring bioluminescence with a luminometer.

STAT phosphorylation assay

PBMCs were treated or not with IT1t (20 μM) overnight. Cells were fixed using Beckman Coulter PerFix EXPOSE Fixation Buffer (10 min at room temperature) and then permeabilized using Beckman Coulter PerFix EXPOSE Permeabilizing Buffer (5 min at 37°C). Cells were stained with PE anti-STAT1 pY701 (clone 4a, 1:5; BD Bioscience) or Alexa Fluor 488 anti-STAT3 pY705 (clone 4/p-STAT3, 1:5; BD Bioscience) and cell surface markers APC-CD3 (clone REA613, 1:30; Miltenyi Biotec) and APC–Alexa Fluor 750–CD14 (clone RM052, 1:30; Beckman Coulter) for 1 hour at room temperature protected from light. Flow cytometry analysis was performed on a Gallios Beckman Coulter flow cytometer. Results were analyzed using Kaluza software v1.3.

Cytokine detection

pDC and tonsil supernatants were tested for multiple cytokine production using the bead assay LEGENDplex Antivirus Human panel (PBL Assay Science, NJ, USA) according to the manufacturer's instructions.

IFN-α in serum and supernatant

As previously reported (*5*), Simoa digital ELISA specific for IFN-α was developed using a Quanterix Homebrew Assay, and two autoantibodies specific for IFN-α were isolated and cloned from two APS1/APECED patients (*59*). The 8H1 antibody clone was used as a capture antibody after coating paramagnetic beads (0.3 mg/ml), and the 12H5 was biotinylated (biotin/Ab ratio = 30:1) and used as the detector. Recombinant IFN-α17/αI (PBL Assay Science) was used as a standard curve after cross-reactivity testing. The limit of detection was calculated by the mean value of all blank runs ± 3 SDs and was 0.23 fg/ml.

RT-qPCR analyses

Total RNA was extracted using the RNeasy Micro kit and was submitted to deoxyribonuclease treatment (Qiagen), following the manufacturer's instructions. RNA concentration and purity were evaluated by spectrophotometry (NanoDrop 2000c, Thermo Fisher Scientific). RNA (500 ng) was reverse-transcribed using the PrimeScript RT Reagent Kit (Perfect Real Time, Takara Bio) in a 10-μl reaction. Real-time PCR reactions were performed in duplicate using Takyon ROX SYBR MasterMix blue deoxythymidine triphosphate (Eurogentec) on an Applied Biosystems QuantStudio 5. Transcripts were quantified using the following program: 3 min at 95°C followed by 35 cycles of 15 s at 95°C, 20 s at 60°C, and 20 s at 72°C. Values for each transcript were normalized to expression levels of RPL13A (60S ribosomal protein L13a) using the $2^{-\Delta\Delta Ct}$ method. Primers used for quantification of transcripts by real time quantitative PCR are indicated below:

RPL13A: forward primer, 5′-AACAGCTCATGAGGCTACGG-3′; reverse primer, 5′-TGGGTCTTGAGGACCTCTGT-3′

TRAIL: forward primer, 5′-GCTGAAGCAGATGCAGGACAA-3′; reverse primer, 5′-TGACGGAGTTGCCACTTGACT-3′

IFNα1: forward primer, 5′-CCAGTTCCAGAAGGCTCCAG-3′; reverse primer, 5′-TCCTCCTGCATCACACAGGC-3′

IFNα4: forward primer, 5′-CCCACAGCCTGGGTAATAGGA-3′; reverse primer, 5′-CAGCAGATGAGTCCTCTGTGC-3′

*IFN*β: forward primer, 5′-TGCTCTCCTGTTGTGCTTCTC-3′; reverse primer, 5′-CAAGCCTCCCATTCAATTGCC-3′
IFNλ1: forward primer, 5′-GGACGCCTTGGAAGAGTCAC-3′; reverse primer, 5′-CTGGTCTAGGACGTCCTCCA-3′
IFNλ2/3: forward primer, 5′-GGGCCTGTATCCAGCCTCAG-3′; reverse primer, 5′-GAGGAGGCGGAAGAGGTTGA-3′
*IFN*γ: forward primer, 5′-GGCAGCCAACCTAAGCAAGAT-3′; reverse primer, 5′-CAGGGTCACCTGACACATTCA-3′
IRF7: forward primer, 5’-CAGATCCAGTCCCAACCAAG-3′; reverse primer, 5′-GTCTCTACTGCCCACCCGTA-3′
MxA: forward primer, 5′-AAGCTGATCCGCCTCCACTT-3′; reverse primer, 5′-TGCAATGCACCCCTGTATACC-3′
TNF-α: forward primer, 5′-GGCGTGGAGCTGAGAGATAAC-3′; reverse primer, 5′-GGTGTGGGTGAGGAGCACAT-3′
CXCL10: forward primer, 5′-CGCTGTACCTGCATCAGCAT-3′; reverse primer, 5′-GCAATGATCTCAACACGTGGAC-3′

IFN stimulated gene RNA expression in PBMCs from patients with lupus

mRNA from treated and nontreated cultured cells were quantified by RT-qPCR using TaqMan probes for *IFI27* (Hs01086370_m1), *IFI44L* (Hs00199115_m1), *ISG15* (Hs00192713_m1), *OAS1* (Hs00973637_m1), *CXCL10* (Hs01124251_m1), *TNFa* (Hs01113624_g1), *IL-6* (Hs00985639_m1), and *IL-17* (Hs00174383_m1); the relative abundance of each target transcript was normalized to the expression level of *HPRT1* (Hs03929096_g1) and assessed with the Applied Biosystems StepOne Software v2.1.

Computational details

An initial structure for AMD3100 was obtained from the ZINC15 database (*60*). The receptor structure was obtained from PDB (Protein Data Bank) ID: 3ODU (chain A) (*20*). The program LeDock (*61*) was used for docking. A cubic box with 40 Å of edge, containing the whole extracellular extreme of the CXCR4 receptor, was used to perform the initial docking screening. We conducted 50 runs of docking simulations, keeping the final pose in each of them. Subsequently, the 50 resulting poses are clustered with a root mean square deviation cutoff of 1 Å. The clusters are ordered according to the binding energy values given by the program force field. The best pose was selected from the most populated cluster among the top 10 scored ones. This structure was further optimized with a simulated annealing procedure. The simulations were performed with NAMD 2.12 (*62*), using the CHARMM36m force field (*63*). Parameters and topologies for the ligands were obtained from SwissParam (*64*). The complexes were placed in a box of explicit solvent with 15 Å of padding in the three dimensions around the complex structures. The model TIP3P was used for the water molecules (*65*). Counter ions were added for neutralization in each system. Long-range electrostatics were evaluated using the PME (particle mesh Ewald) method (*66*). The solvent was initially equilibrated to the box dimensions along 150 ps of NVT simulation at 300 K with the complex structure fixed in its initial geometry. Next, 1 ns of NPT simulation was performed with harmonic constraints on the protein and ligand's atoms. Langevin dynamics (*67*) was used to control the temperature and pressure of the system at 300 K and 1 atm, respectively. Then, a local optimization was performed with short cycles of a simulated annealing (SA) procedure. The SA protocol was composed of five cycles, involving a heating ramp between 300 and 350 K for 1 ns, then a cooling ramp back to 300 K for 1 ns, and, afterward, 1 ns of re-equilibration at 300 K. In total, the protocol involved 15 ns of optimization. The last step involved the equilibration at 300 K. The receptor's backbone was kept fixed during the simulation using a harmonic restraint. Side chains, ligand, and solvent were allowed to move freely.

In vivo treatment of mice

Animal experiments were performed blindly by Washington Biotechnology, Inc. The animals were housed in a temperature- and humidity-controlled room with 12-hour light/dark cycles with food and water ad libitum. The Washington Biotechnology, Inc. Animal Care and Use Committee reviewed and approved all mouse experiments (IACUC no. 17-006). Animal welfare and experimental protocols strictly complied with the *Guide for the Care and Use of Laboratory Animals* and the ethics and regulations. For pristane injection, each mouse in all groups was intraperitoneally injected with 0.5 ml of pristane (cat no. P9622, Sigma-Aldrich, BioReagent). Prednisolone (4.5 mg; P4153, Sigma-Aldrich) was dissolved in 3 ml of PBS to prepare a solution (1.5 mg/ml). All mice in group 2 were treated daily with prednisolone (15 mg/ml oral gavage). IT1t was dissolved in PBS and intraperitoneally injected daily at 3 mg/kg (mpK), 10, or 30 mpK (groups 3 to 5). ELISA was performed using the following kit according to the manufacturer's recommendation: TNF-α ELISA kit (cat no. MTA00B, R&D Systems), IL-1β ELISA kit (cat no. MLB00C, R&D Systems), IL-17 ELISA kit (cat no. M1700, R&D Systems), TRAIL ELISA kit (cat. no. ELM-TRAIL-1, RayBiotech), and dsDNA (IgM) ELISA Kit (cat. no. 5120, Alpha Diagnostic). For histology, formalin-fixed samples of each kidney from mice were received by HistoTox Labs and processed routinely. One slide per block was sectioned and stained with hematoxylin and eosin. Glass slides were evaluated by a board-certified veterinary pathologist, using light microscopy. Glomerulonephritis was characterized by slight thickening of mesangial matrix or mesangial hypercellularity (>3 nuclei per segment).

Nanostring gene expression analysis

Total RNA was extracted from isolated pDCs of controls and patients and was diluted with ribonuclease-free water at 20 ng/μl, and 100 ng (5 μl) of each sample was analyzed using the Human Immunology kit v2 and Nanostring Counter. Each sample was analyzed in a separate multiplexed reaction including, in each, eight negative probes and six serial concentrations of positive control probes. Data were imported into nSolver analysis software (version 2.5) for quality checking and normalization of data according to NanoString analysis guidelines, using positive probes and housekeeping genes. For analysis, mRNA expression levels were log-transformed and mean-centered per donor (when applicable) before hierarchical clustering (Qlucore Omics Explorer version 3.1). Up-regulated genes from the heat map shown in Fig. 2B were classified with respect to their known link to IFN signaling or functional promoter. Identification of ISGs was made using the database from Shaw *et al.* (*68*) (http://isg.data.cvr.ac.uk/). Promoters of the remaining genes were identified on the basis of the "Molecular Signatures Database v6.2" C3 from the Broad Institute (http://software.broadinstitute.org/gsea/msigdb/index.jsp) (*69*, *70*). When multiple transcription factors were identified for the same gene, the one in common with other genes was chosen in priority for the graphical representation.

Statistical analysis

Cellular data are shown as median and min/max. Datasets were analyzed by Kruskal-Wallis test with Dunn's post hoc correction. Univariate distributions of flow cytometry data were performed by probability

binning in 300 bins using FlowJo software. Animal data are shown as mean ± SEM. Datasets were analyzed using two-way analysis of variance (ANOVA) with Bonferroni post hoc comparison (cytokine concentration in time course). GraphPad Prism 5 (GraphPad Software, San Diego, CA) was used for data analysis and preparation of all graphs. *P* values less than 0.05 were considered to be statistically significant.

SUPPLEMENTARY MATERIALS

Supplementary material for this article is available at http://advances.sciencemag.org/cgi/content/full/5/7/eaav9019/DC1

Fig. S1. AMD3100 and IT1t bind to CXCR4 and are not toxic.
Fig. S2. IT1t controls TLR7-mediated inflammation in HIV-stimulated pDCs.
Fig. S3. IT1t inhibits pDC activation through CXCR4 engagement.
Fig. S4. Genes from the R848 stimulated group are significantly enrich in ISG.
Table S1. Clinical information of recruited patients.

REFERENCES AND NOTES

1. L. B. Ivashkiv, L. T. Donlin, Regulation of type I interferon responses. *Nat. Rev. Immunol.* **14**, 36–49 (2014).
2. X. Dagenais-Lussier, H. Loucif, A. Murira, X. Laulhé, S. Stäger, A. Lamarre, J. van Grevenynghe, Seustained IFN-I expression during established persistent viral infection: A "bad seed" for protective immunity. *Viruses* **10**, 12 (2017).
3. M. P. Rodero, Y. J. Crow, Type I interferon-mediated monogenic autoinflammation: The type I interferonopathies, a conceptual overview. *J. Exp. Med.* **213**, 2527–2538 (2016).
4. R. Banchereau, S. Hong, B. Cantarel, N. Baldwin, J. Baisch, M. Edens, A.-M. Cepika, P. Acs, J. Turner, E. Anguiano, P. Vinod, S. Khan, G. Obermoser, D. Blankenship, E. Wakeland, L. Nassi, A. Gotte, M. Punaro, Y.-J. Liu, J. Banchereau, J. Rossello-Urgell, T. Wright, V. Pascual, Personalized immunomonitoring uncovers molecular networks that stratify lupus patients. *Cell* **165**, 551–565 (2016).
5. M. P. Rodero, J. Decalf, V. Bondet, D. Hunt, G. I. Rice, S. Werneke, S. L. McGlasson, M.-A. Alyanakian, B. Bader-Meunier, C. Barnerias, N. Bellon, A. Belot, C. Bodemer, T. A. Briggs, I. Desguerre, M.-L. Frémond, M. Hully, A. M. J. M. van den Maagdenberg, I. Melki, I. Meyts, L. Musset, N. Pelzer, P. Quartier, G. M. Terwindt, J. Wardlaw, S. Wiseman, F. Rieux-Laucat, Y. Rose, B. Neven, C. Hertel, A. Hayday, M. L. Albert, F. Rozenberg, Y. J. Crow, D. Duffy, Detection of interferon alpha protein reveals differential levels and cellular sources in disease. *J. Exp. Med.* **214**, 1547–1555 (2017).
6. G. Grouard, M.-C. Rissoan, L. Filgueira, I. Durand, J. Banchereau, Y.-J. Liu, The enigmatic plasmacytoid T cells develop into dendritic cells with interleukin (IL)-3 and CD40-ligand. *J. Exp. Med.* **185**, 1101–1111 (1997).
7. M. Colonna, M. Cella, Crosspresentation: Plasmacytoid dendritic cells are in the business. *Immunity* **27**, 419–421 (2007).
8. F. P. Siegal, N. Kadowaki, M. Shodell, P. A. Fitzgerald-Bocarsly, K. Shah, S. Ho, S. Antonenko, Y.-J. Liu, The nature of the principal type I interferon-producing cells in human blood. *Science* **284**, 1835–1837 (1999).
9. D. Jarrossay, G. Napolitani, M. Colonna, F. Sallusto, A. Lanzavecchia, Specialization and complementarity in microbial molecule recognition by human myeloid and plasmacytoid dendritic cells. *Eur. J. Immunol.* **31**, 3388–3393 (2001).
10. N. Kadowaki, Y.-J. Liu, Natural type I interferon-producing cells as a link between innate and adaptive immunity. *Hum. Immunol.* **63**, 1126–1132 (2002).
11. M. Gandini, C. Gras, E. L. Azeredo, L. M. de Oliveira Pinto, N. Smith, P. Despres, R. V. da Cunha, L. J. de Souza, C. F. Kubelka, J.-P. Herbeuval, Dengue virus activates membrane TRAIL relocalization and IFN-α production by human plasmacytoid dendritic cells in vitro and in vivo. *PLOS Negl. Trop. Dis.* **7**, e2257 (2013).
12. A. W. Hardy, D. R. Graham, G. M. Shearer, J. P. Herbeuval, HIV turns plasmacytoid dendritic cells (pDC) into TRAIL-expressing killer pDC and down-regulates HIV coreceptors by Toll-like receptor 7-induced IFN-alpha. *Proc. Natl. Acad. Sci. U.S.A.* **104**, 17453–17458 (2007).
13. H. Hemmi, O. Takeuchi, T. Kawai, T. Kaisho, S. Sato, H. Sanjo, M. Matsumoto, K. Hoshino, H. Wagner, K. Takeda, S. Akira, A Toll-like receptor recognizes bacterial DNA. *Nature* **408**, 740–745 (2000).
14. M. Swiecki, M. Colonna, The multifaceted biology of plasmacytoid dendritic cells. *Nat. Rev. Immunol.* **15**, 471–485 (2015).
15. L. Rönnblom, V. Pascual, The innate immune system in SLE: Type I interferons and dendritic cells. *Lupus* **17**, 394–399 (2008).
16. K. Sakata, S. Nakayamada, Y. Miyazaki, S. Kubo, A. Ishii, K. Nakano, Y. Tanaka, Up-regulation of TLR7-mediated IFN-α production by plasmacytoid dendritic cells in patients with systemic lupus erythematosus. *Front. Immunol.* **9**, 1957 (2018).
17. B. F. Chong, C. Mohan, Targeting the CXCR4/CXCL12 axis in systemic lupus erythematosus. *Expert Opin. Ther. Targets* **13**, 1147–1153 (2009).
18. A. Wang, A.-M. Fairhurst, K. Tus, S. Subramanian, Y. Liu, F. Lin, P. Igarashi, X. J. Zhou, F. Batteux, D. Wong, E. K. Wakeland, C. Mohan, CXCR4/CXCL12 hyperexpression plays a pivotal role in the pathogenesis of lupus. *J. Immunol.* **182**, 4448–4458 (2009).
19. N. Smith, N. Pietrancosta, S. Davidson, J. Dutrieux, L. Chauveau, P. Cutolo, M. Dy, D. Scott-Algara, B. Manoury, O. Zirafi, I. McCort-Tranchepain, T. Durroux, F. Bachelerie, O. Schwartz, J. Münch, A. Wack, S. Nisole, J.-P. Herbeuval, Natural amines inhibit activation of human plasmacytoid dendritic cells through CXCR4 engagement. *Nat. Commun.* **8**, 14253 (2017).
20. B. Wu, E. Y. T. Chien, C. D. Mol, G. Fenalti, W. Liu, V. Katritch, R. Abagyan, A. Brooun, P. Wells, F. C. Bi, D. J. Hamel, P. Kuhn, T. M. Handel, V. Cherezov, R. C. Stevens, Structures of the CXCR4 chemokine GPCR with small-molecule and cyclic peptide antagonists. *Science* **330**, 1066–1071 (2010).
21. J. F. Dipersio, I. N. Micallef, P. J. Stiff, B. J. Bolwell, R. T. Maziarz, E. Jacobsen, A. Nademanee, J. McCarty, G. Bridger, G. Calandra, Phase III prospective randomized double-blind placebo-controlled trial of plerixafor plus granulocyte colony-stimulating factor compared with placebo plus granulocyte colony-stimulating factor for autologous stem-cell mobilization and transplantation for patients with non-hodgkin's lymphoma. *J. Clin. Oncol.* **27**, 4767–4773 (2009).
22. D. J. Scholten, M. Canals, D. Maussang, L. Roumen, M. J. Smit, M. Wijtmans, C. de Graaf, H. F. Vischer, R. Leurs, Pharmacological modulation of chemokine receptor function. *Br. J. Pharmacol.* **165**, 1617–1643 (2012).
23. M. M. Rosenkilde, L.-O. Gerlach, S. Hatse, R. T. Skerlj, D. Schols, G. J. Bridger, T. W. Schwartz, Molecular mechanism of action of monocyclam versus bicyclam non-peptide antagonists in the CXCR4 chemokine receptor. *J. Biol. Chem.* **282**, 27354–27365 (2007).
24. M. M. Rosenkilde, L.-O. Gerlach, J. S. Jakobsen, R. T. Skerlj, G. J. Bridger, T. W. Schwartz, Molecular mechanism of AMD3100 antagonism in the CXCR4 receptor: Transfer of binding site to the CXCR3 receptor. *J. Biol. Chem.* **279**, 3033–3041 (2004).
25. G. A. Donzella, D. Schols, S. W. Lin, J. A. Esté, K. A. Nagashima, P. J. Maddon, G. P. Allaway, T. P. Sakmar, G. Henson, E. DeClercq, J. P. Moore, AMD3100, a small molecule inhibitor of HIV-1 entry via the CXCR4 co-receptor. *Nat. Med.* **4**, 72–77 (1998).
26. G. Thoma, M. B. Streiff, J. Kovarik, F. Glickman, T. Wagner, C. Beerli, H.-G. Zerwes, Orally bioavailable isothioureas block function of the chemokine receptor CXCR4 in vitro and in vivo. *J. Med. Chem.* **51**, 7915–7920 (2008).
27. N. Smith, P. O. Vidalain, S. Nisole, J. P. Herbeuval, An efficient method for gene silencing in human primary plasmacytoid dendritic cells: Silencing of the TLR7/IRF-7 pathway as a proof of concept. *Sci. Rep.* **6**, 29891 (2016).
28. J. P. Herbeuval, J. Nilsson, A. Boasso, A. W. Hardy, M. J. Kruhlak, S. A. Anderson, M. J. Dolan, M. Dy, J. Andersson, G. M. Shearer, Differential expression of IFN-alpha and TRAIL/DR5 in lymphoid tissue of progressor versus nonprogressor HIV-1-infected patients. *Proc. Natl. Acad. Sci. U.S.A.* **103**, 7000–7005 (2006).
29. J.-P. Herbeuval, A. Boasso, J.-C. Grivel, A. W. Hardy, S. A. Anderson, M. J. Dolan, C. Chougnet, J. D. Lifson, G. M. Shearer, TNF-related apoptosis-inducing ligand (TRAIL) in HIV-1-infected patients and its in vitro production by antigen-presenting cells. *Blood* **105**, 2458–2464 (2005).
30. A. Kaul, C. Gordon, M. K. Crow, Z. Touma, M. B. Urowitz, R. van Vollenhoven, G. Ruiz-Irastorza, G. Hughes, Systemic lupus erythematosus. *Nat. Rev. Dis. Primers* **2**, 16039 (2016).
31. V. Salvi, V. Gianello, S. Busatto, P. Bergese, L. Andreoli, U. D'Oro, A. Zingoni, A. Tincani, S. Sozzani, D. Bosisio, Exosome-delivered microRNAs promote IFN-alpha secretion by human plasmacytoid DCs via TLR7. *JCI Insight* **3**, 98204 (2018).
32. G. Murayama, N. Furusawa, A. Chiba, K. Yamaji, N. Tamura, S. Miyake, Enhanced IFN-alpha production is associated with increased TLR7 retention in the lysosomes of palasmacytoid dendritic cells in systemic lupus erythematosus. *Arthritis Res. Ther.* **19**, 234 (2017).
33. V. Sisirak, D. Ganguly, K. L. Lewis, C. Couillault, L. Tanaka, S. Bolland, V. D'Agati, K. B. Elkon, B. Reizis, Genetic evidence for the role of plasmacytoid dendritic cells in systemic lupus erythematosus. *J. Exp. Med.* **211**, 1969–1976 (2014).
34. C. Guiducci, M. Gong, Z. Xu, M. Gill, D. Chaussabel, T. Meeker, J. H. Chan, T. Wright, M. Punaro, S. Bolland, V. Soumelis, J. Banchereau, R. L. Coffman, V. Pascual, F. J. Barrat, TLR recognition of self nucleic acids hampers glucocorticoid activity in lupus. *Nature* **465**, 937–941 (2010).
35. H. Zhuang, C. Szeto, S. Han, L. Yang, W. H. Reeves, Animal models of interferon signature positive lupus. *Front. Immunol.* **6**, 291 (2015).
36. E. Savarese, C. Steinberg, R. D. Pawar, W. Reindl, S. Akira, H.-J. Anders, A. Krug, Requirement of Toll-like receptor 7 for pristane-induced production of autoantibodies and development of murine lupus nephritis. *Arthritis Rheum.* **58**, 1107–1115 (2008).
37. X. Chen, R. Cui, R. Li, H. Lin, Z. Huang, L. Lin, Development of pristane induced mice model for lupus with atherosclerosis and analysis of TLR expression. *Clin. Exp. Rheumatol.* **34**, 600–608 (2016).
38. M. Lucas-Hourani, D. Dauzonne, P. Jorda, G. Cousin, A. Lupan, O. Helynck, G. Caignard, G. Janvier, G. André-Leroux, S. Khiar, N. Escriou, P. Desprès, Y. Jacob, H. Munier-Lehmann, F. Tangy, P.-O. Vidalain, Inhibition of pyrimidine biosynthesis pathway suppresses viral growth through innate immunity. *PLOS Pathog.* **9**, e1003678 (2013).

39. M. J. Mirzayan, R. E. Schmidt, T. Witte, Prognostic parameters for flare in systemic lupus erythematosus. *Rheumatology* **39**, 1316–1319 (2000).
40. S. Caielli, S. Athale, B. Domic, E. Murat, M. Chandra, R. Banchereau, J. Baisch, K. Phelps, S. Clayton, M. Gong, T. Wright, M. Punaro, K. Palucka, C. Guiducci, J. Banchereau, V. Pascual, Oxidized mitochondrial nucleoids released by neutrophils drive type I interferon production in human lupus. *J. Exp. Med.* **213**, 697–713 (2016).
41. S. S. Diebold, T. Kaisho, H. Hemmi, S. Akira, C. Reis e Sousa, Innate antiviral responses by means of TLR7-mediated recognition of single-stranded RNA. *Science* **303**, 1529–1531 (2004).
42. S. S. Diebold, M. Montoya, H. Unger, L. Alexopoulou, P. Roy, L. E. Haswell, A. Al-Shamkhani, R. Flavell, P. Borrow, C. Reis e Sousa, Viral infection switches non-plasmacytoid dendritic cells into high interferon producers. *Nature* **424**, 324–328 (2003).
43. J. Banchereau, V. Pascual, Type I interferon in systemic lupus erythematosus and other autoimmune diseases. *Immunity* **25**, 383–392 (2006).
44. T. B. Niewold, Type I interferon in human autoimmunity. *Front. Immunol.* **5**, 306 (2014).
45. L. Cheng, J. Ma, J. Li, D. Li, G. Li, F. Li, Q. Zhang, H. Yu, F. Yasui, C. Ye, L. C. Tsao, Z. Hu, L. Su, L. Zhang, Blocking type I interferon signaling enhances T cell recovery and reduces HIV-1 reservoirs. *J. Clin. Invest.* **127**, 269–279 (2017).
46. S. G. Deeks, P. M. Odorizzi, R. P. Sekaly, The interferon paradox: Can inhibiting an antiviral mechanism advance an HIV cure? *J. Clin. Invest.* **127**, 103–105 (2017).
47. A. Zhen, V. Rezek, C. Youn, B. Lam, N. Chang, J. Rick, M. Carrillo, H. Martin, S. Kasparian, P. Syed, N. Rice, D. G. Brooks, S. G. Kitchen, Targeting type I interferon-mediated activation restores immune function in chronic HIV infection. *J. Clin. Invest.* **127**, 260–268 (2017).
48. S. Luo, Y. Wang, M. Zhao, Q. Lu, The important roles of type I interferon and interferon-inducible genes in systemic lupus erythematosus. *Int. Immunopharmacol.* **40**, 542–549 (2016).
49. L. Bennett, A. K. Palucka, E. Arce, V. Cantrell, J. Borvak, J. Banchereau, V. Pascual, Interferon and granulopoiesis signatures in systemic lupus erythematosus blood. *J. Exp. Med.* **197**, 711–723 (2003).
50. V. Pascual, J. Banchereau, A. K. Palucka, The central role of dendritic cells and interferon-alpha in SLE. *Curr. Opin. Rheumatol.* **15**, 548–556 (2003).
51. R. Felten, E. Dervovic, F. Chasset, J. E. Gottenberg, J. Sibilia, F. Scher, L. Arnaud, The 2018 pipeline of targeted therapies under clinical development for systemic lupus erythematosus: A systematic review of trials. *Autoimmun. Rev.* **17**, 781–790 (2018).
52. S. L. Rowland, J. M. Riggs, S. Gilfillan, M. Bugatti, W. Vermi, R. Kolbeck, E. R. Unanue, M. A. Sanjuan, M. Colonna, Early, transient depletion of plasmacytoid dendritic cells ameliorates autoimmunity in a lupus model. *J. Exp. Med.* **211**, 1977–1991 (2014).
53. M. Hasan, N. Dobbs, S. Khan, M. A. White, E. K. Wakeland, Q.-Z. Li, N. Yan, Cutting edge: Inhibiting TBK1 by compound II ameliorates autoimmune disease in mice. *J. Immunol.* **195**, 4573–4577 (2015).
54. H. Zhuang, S. Han, Y. Xu, Y. Li, H. Wang, L.-J. Yang, W. H. Reeves, Toll-like receptor 7-stimulated tumor necrosis factor α causes bone marrow damage in systemic lupus erythematosus. *Arthritis Rheum.* **66**, 140–151 (2014).
55. P. Y. Lee, J. S. Weinstein, D. C. Nacionales, P. O. Scumpia, Y. Li, E. Butfiloski, N. van Rooijen, L. Moldawer, M. Satoh, W. H. Reeves, A novel type I IFN-producing cell subset in murine lupus. *J. Immunol.* **180**, 5101–5108 (2008).
56. B. Debnath, S. Xu, F. Grande, A. Garofalo, N. Neamati, Small molecule inhibitors of CXCR4. *Theranostics* **3**, 47–75 (2013).
57. R. K. Mishra, A. K. Shum, L. C. Platanias, R. J. Miller, G. E. Schiltz, Discovery and characterization of novel small-molecule CXCR4 receptor agonists and antagonists. *Sci. Rep.* **6**, 30155 (2016).
58. K. Nujić, M. Banjanac, V. Munić, D. Polančec, V. Eraković Haber, Impairment of lysosomal functions by azithromycin and chloroquine contributes to anti-inflammatory phenotype. *Cell. Immunol.* **279**, 78–86 (2012).
59. S. Meyer, M. Woodward, C. Hertel, P. Vlaicu, Y. Haque, J. Kärner, A. Macagno, S. C. Onuoha, D. Fishman, H. Peterson, K. Metsküla, R. Uibo, K. Jäntti, K. Hokynar, A. S. B. Wolff; APECED patient collaborative, K. Krohn, A. Ranki, P. Peterson, K. Kisand, A. Hayday, AIRE-deficient patients harbor unique high-affinity disease-ameliorating autoantibodies. *Cell* **166**, 582–595 (2016).
60. T. Sterling, J. J. Irwin, ZINC 15—Ligand discovery for everyone. *J. Chem. Inf. Model.* **55**, 2324–2337 (2015).
61. H. Zhao, A. Caflisch, Discovery of ZAP70 inhibitors by high-throughput docking into a conformation of its kinase domain generated by molecular dynamics. *Bioorg. Med. Chem. Lett.* **23**, 5721–5726 (2013).
62. J. C. Phillips, R. Braun, W. Wang, J. Gumbart, E. Tajkhorshid, E. Villa, C. Chipot, R. D. Skeel, L. Kalé, K. Schulten, Scalable molecular dynamics with NAMD. *J. Comput. Chem.* **26**, 1781–1802 (2005).
63. J. Huang, S. Rauscher, G. Nawrocki, T. Ran, M. Feig, B. L. de Groot, H. Grubmüller, A. D. MacKerell Jr., CHARMM36m: An improved force field for folded and intrinsically disordered proteins. *Nat. Methods* **14**, 71–73 (2017).
64. V. Zoete, M. A. Cuendet, A. L. Grosdidier, O. Michielin, SwissParam: A fast force field generation tool for small organic molecules. *J. Comput. Chem.* **32**, 2359–2368 (2011).
65. P. Mark, L. Nilsson, Structure and dynamics of the TIP3P, SPC, and SPC/E water models at 298 K. *J. Phys. Chem.* **105**, 9954–9960 (2001).
66. R. J. Shattock, B. F. Haynes, B. Pulendran, J. Flores, J. Esparza, Improving defences at the portal of HIV entry: Mucosal and innate immunity. *PLOS Med.* **5**, e81 (2008).
67. J. A. Izaguirre, D. P. Catarello, J. M. Wozniak, R. D. Skeel, Langevin stabilization of molecular dynamics. *J. Chem. Phys.* **114**, 2090–2098 (2001).
68. A. E. Shaw, J. Hughes, Q. Gu, A. Behdenna, J. B. Singer, T. Dennis, R. J. Orton, M. Varela, R. J. Gifford, S. J. Wilson, M. Palmarini, Fundamental properties of the mammalian innate immune system revealed by multispecies comparison of type I interferon responses. *PLOS Biol.* **15**, e2004086 (2017).
69. X. Xie, J. Lu, E. J. Kulbokas, T. R. Golub, V. Mootha, K. Lindblad-Toh, E. S. Lander, M. Kellis, Systematic discovery of regulatory motifs in human promoters and 3′ UTRs by comparison of several mammals. *Nature* **434**, 338–345 (2005).
70. A. Subramanian, P. Tamayo, V. K. Mootha, S. Mukherjee, B. L. Ebert, M. A. Gillette, A. Paulovich, S. L. Pomeroy, T. R. Golub, E. S. Lander, J. P. Mesirov, Gene set enrichment analysis: A knowledge-based approach for interpreting genome-wide expression profiles. *Proc. Natl. Acad. Sci. U.S.A.* **102**, 15545–15550 (2005).

Acknowledgments: We thank S. Dupuy from the Common Service of Flux Cytometry (S2C) of Paris Descartes University. We also thank N. Pietrancosta for providing us with some IT1t for the mice study. Furthermore, we thank J. Bess and J. Lifson for providing us with the inactivated purified HIV-1 viruses. **Funding:** This work was supported by the Agence National de la Recherche sur le SIDA et les Hépatites ANRS (to J.-P.H.) for the experiments and N.B. Fellowship (AAP 2017-166). N.S. acknowledges support from the ANRS for Fellowship (AAP 2016-1), the European Molecular Biology Organization (EMBO) for Fellowship (LT-834-2017), the start-up funding program "Baustein" of the Medical Faculty of Ulm University (LSBN.0147), and the Deutsche Forschungsgemeinschaft (DFG; SM 544/1-1). This work was also supported by SATT IDF Innov (www.idfinnov.com) through the project under grant no. 303. D.D. acknowledges support from the Agence National de Recherche ANR (CE17001002) and ImmunoQure for provision of mAbs for Simoa assays. J.M. acknowledges support from DFG (MU3115-8/1 and CRC1279). A.-S.K and Y.D. acknowledge support from the Société Nationale Française de Médecine Interne (SNFMI), from Hôpitaux Universitaires de Strasbourg (HUS), and from EU-funded (ERDF) project Interreg V "RARENET". A.-S.K. also acknowledges support from the French Ministry of Health (PHRC IR 2011). S.N. has benefited from support by the LABEX EpiGenMed, an "Investissements d'avenir" program (reference, ANR-10-LABX-12-01). B.J. acknowledges the BSD grant (Budgetantrag, 11225783). E.S.G. acknowledges the support of the German Research Foundation (DFG) under Germany's Excellence Strategy—EXC-2033—Projektnummer 390677874, the CRC1279, and the Boehringer-Ingelheim Foundation (Plus-3 Grant). These experiments used reagents provided by the AIDS and Cancer Virus Program, Biological Products Core Laboratory, Frederick National Laboratory for Cancer Research, supported with federal funds from the National Cancer Institute, National Institutes of Health, under contract HHSN261200800001E. **Author contributions:** N.S., M.P.R., D.D., and J.-P.H. designed research; N.S., N.B., S.N., M.P.R., M.H., and Y.R. performed the experiments; V.B. performed the SIMOA dosage; B.C. performed the nanostring experiments. Y.B.R.-B. and E.S.G. performed the molecular modeling and analysis. N.S., M.P.R., N.B., V.B., B.C., S.N., D.D., and J.-P.H. analyzed research; B.B-M., C.B., Y.R., V.B., P.Q., A.-S.K., and Y.D. gave access to patients' material; B.M. performed the statistical analysis; B.J. and N.L. gave access to tonsils and healthy donors' blood; F.K. and J.M. provided material and took part in scientific discussion; N.S., D.D., and J.M. contributed to writing the paper; and M.P.R. and J.-P.H. wrote the paper. **Competing interests:** N.S. and J.-P.H. are inventors on a patent related to this work filed by the Centre National de la Recherche Scientifique (CNRS) and the Université Paris Descartes (no. WO 2017/216368 Al, filed 16 June 2017, published 21 December 2017). The authors declare that they have no other competing interests. **Data and materials availability:** All data needed to evaluate the conclusions in the paper are present in the paper and/or the Supplementary Materials. The mAb for the Simoa IFN-α was obtained under a material transfer agreement. Requests for the mAb can be made to ImmunoQure AG directly. Additional data related to this paper may be requested from the authors.

Submitted 30 October 2018
Accepted 6 June 2019
Published 10 July 2019
10.1126/sciadv.aav9019

Citation: N. Smith, M. P. Rodero, N. Bekaddour, V. Bondet, Y. B. Ruiz-Blanco, M. Harms, B. Mayer, B. Bader-Meunier, P. Quartier, C. Bodemer, V. Baudouin, Y. Dieudonné, F. Kirchhoff, E. Sanchez Garcia, B. Charbit, N. Leboulanger, B. Jahrsdörfer, Y. Richard, A.-S. Korganow, J. Münch, S. Nisole, D. Duffy, J.-P. Herbeuval, Control of TLR7-mediated type I IFN signaling in pDCs through CXCR4 engagement—A new target for lupus treatment. *Sci. Adv.* **5**, eaav9019 (2019).